5-1-2012

THE USE OF STOMP TO EVALUATE THE IMPACT OF HETEROGENEITY ON LNAPL POOL CONFIGURATION

Saroj Kandel

Southern Illinois University Carbondale, sonique_saroj@hotmail.com

Follow this and additional works at: http://opensiuc.lib.siu.edu/theses

THE USE OF STOMP TO EVALUATE THE IMPACT OF

HETEROGENEITY ON LNAPL POOL CONFIGURATION

By

Saroj Kandel

B.S., Tribhuvan University, 2008

A Thesis

Submitted in partial fulfillment of the requirements for the degree of

Master of Science

Department of Civil and Environmental Engineering

Graduate School

Southern Illinois University Carbondale

May 2012

THESIS APPROVAL

THE USE OF STOMP TO EVALUATE THE IMPACT OF HETEROGENEITY
ON LNAPL POOL CONFIGURATION

By

Saroj Kandel

A Thesis Submitted in Partial

Fulfillment of the Requirements for the Degree of

Master of Science

in the field of Civil and Environmental Engineering

Approved by:

Dr. Lizette R. Chevalier, Chair

Dr. Bruce A. Devantier

Dr. Xingmao Ma

Graduate School

Southern Illinois University Carbondale

February 6, 2012

AN ABSTRACT OF THE THESIS OF

SAROJ KANDEL, for the Masters of Science degree in CIVIL ENGINEERING, presented on February 6, 2012, at Southern Illinois University Carbondale.

TITLE: THE USE OF STOMP TO EVALUATE THE IMPACT OF HETEROGENEITY ON LNAPL POOL CONFIGURATION

MAJOR PROFESSOR: Dr. Lizette R. Chevalier

Subsurface contamination by light non-aqueous phase liquid (LNAPL) is a widespread problem. A common LNAPL contamination is gasoline from leaking underground storage tanks (LUST). Heterogeneities in the media properties play a crucial role for defining the LNAPL movement and distribution in the subsurface. Hence, enhanced understanding of light non-aqueous phase liquid (LNAPL) movement into heterogeneous porous media is important for the effective design of remediation strategies. Numerical simulations are important tools for the understanding of subsurface multi-phase flow and transport processes. The numerical simulator Subsurface Transport Over Multiple Phases (STOMP) was used to simulate two-phase flow in porous media in an unconfined aquifer. The simulations was conducted with the water-oil (w-*o*) mode of the of the multi-fluid flow simulator STOMP. Two different patterns of layered heterogeneity were used for the simulation of LNAPL movement in an unconfined aquifer. The first pattern (P1: coarse − fine − coarse) showed the maximum LNAPL distribution occurred in the capillary fringe region just above the water table in the fine sand layer region. The second pattern (P2: fine − coarse −fine) showed the LNAPL spreading just above the capillary fringe region not even reaching the capillary zone. The main controlling factor determining the final LNAPL movement and distribution in the layered heterogeneous pattern (P1: coarse − fine − coarse) and (P2: fine -coarse − fine) was capillary pressure and permeability of the media present.

DEDICATION

I dedicate this work to:

- My mother Shanta Kandel and my father Bharat Babu Kandel for their love and care.

- My sisters: Sarala, and Sudipna.

ACKNOWLEDGEMENTS

TABLE OF CONTENTS

LIST OF TABLES

LIST OF FIGURES

CHAPTER 1

INTRODUCTION

Subsurface contamination by non-aqueous phase liquid (NAPL) is a widespread problem. The leaking from underground storage tanks (USTs) and pipelines, hazardous waste sites and surface spills are the general sources of ground water contamination from non-aqueous phase liquid (NAPL). A non-aqueous phase liquid (NAPL) is petroleum based compound that is immiscible with water. A NAPL with density less than water is classified as a light non-aqueous phase liquid (LNAPL), and a NAPL with density higher than water is classified as a dense non-aqueous phase liquid (DNAPL). LNAPL migrate through an unconfined aquifer and pool above the water saturated pores of the capillary fringe whereas DNAPL will continue to move downward through the saturated soil. If there is a sufficient volume of DNAPL, it will pool at an impermeable boundary. As such, NAPL released into subsurface can be found pooled (free phase), as a residual in an unconfined aquifer, or trapped in isolated blobs in the saturated region. Direct human exposure to NAPL is rare, but NAPL in the subsurface is a persistent source for soil and ground water contamination (Kechavarzi et al., 2005). A common LNAPL contamination is gasoline from leaking underground storage tanks (LUST). More than 397,000 confirmed cases of leaking underground storage tanks (LUSTs) have been reported in the United States of America (U.S.EPA, 2000). The maximum contamination level (MCL) allowed for drinking water purpose set up by the Environmental protection Agency (EPA) are listed in Table 1.1.

Table 1.1: Densities, water solubility and maximum contaminants level

NAPL	Density (mg/L) at 20° C	Water solubility (mg/L)	MCL (mg/L)
Benzene	0.879^a	1750^b	0.005^c
Ethyl Benzene	0.867^a	152^b	0.7^c
p-Xylene	0.8611^a	198^b	10^c
Tetrachloroethene	1.6227^a	150^b	0.005^c
Toulene	0.8669^a	535^b	1^c
1,1,1 Trichloroethane	1.339^a	1500^b	0.2^c
Trichloroethane	1.467^a	1100^a	0.005^c

a: Davis and Cornwell,1998, *b*: Mercer and Cohen,1990, *c*: EPA , 2009

Since the maximum contamination levels (MCL) are lower than the solubility of the contaminant in ground water, highly efficient and sophisticated remediation technologies are required to alleviate the long term source of groundwater pollution from NAPLs. Over the past decades several technologies have been developed for NAPLs remediation. The most commonly used method is pump and treat, in which the groundwater is pumped out from the site, treated on the surface to remove the contaminant and finally re-injected (Mackay and Cherry, 1989). Other remediation methods include injection of surfactants (Pennell et al., 1994; West and Harwell, 1992), co-solvents, such as alcohols (Pinal et al., 1990), and air- sparging in the ground water.

However, the efficiency of pump-and-treat was largely affected by rate limited dissolution, heterogeneity in subsurface characteristics, and non-uniform distribution behavior of

NAPL. All these factors play roles in increasing remediation time and cost if proper care is not taken before remediation (Abriola et al., 2005). The study of NAPL spills in the subsurface is complex. The design of effective remediation techniques for light non aqueous phase liquid (LNAPL) is based on the predication of its geometry and position in the subsurface (Chevalier 1998; Schroth et al., 1995). To study NAPL flow and design of remediation technology, different laboratory setup has been used, where properties of NAPL were studied in different porous media using different pore size (Pantazidou and Sitar 1993; Schroth et al., 1995; Schroth et al., 1998; Wipfler et al., 2004). These studies were mainly focused on dissolution (Dobson et al., 2007; Seyedabbasi et al., 2008), flow pattern, entrapment, and distribution of NAPL in three phases or mass transfer. The distribution of grain size and thus pore sizes determines the NAPL migration and entrapment phenomena on a complex NAPL distribution   (Illangasekare et al., 1995; Kueper et al., 1989). The study of non-aqueous phase liquid (NAPL) transport in ground water requires a correct description of multiphase flow in porous media. Such description includes a number of material dependent parameters, including relationship between capillary pressure, saturation, and relative permeability (p-*S-k)* relationships. The determination of these relationships is often a difficult task, and is more complex when material under study is heterogeneous (Ataie-Ashtiani et al., 2001). Such heterogeneity in material properties can significantly affect the overall flow properties of the system, including the spreading behavior of non-aqueous phase liquids (Ataie-Ashtiani et al., 2001) . These heterogeneities can also produce a localized pool of NAPL.

Most of the laboratory and numerical experiments on NAPLs were completed in one dimensional (1-D) columns (Chao et al., 2000; Rimmer et al., 1996). Due to the constraint in

flow boundaries, researchers have used two dimensional (2-D) tanks made of glass, metal, or 2-D numerical simulation.

Numerical simulations are important tools for the understanding of subsurface multi-phase flow and transport processes. A number of numerical simulators have been developed to model NAPL flow and transport in the subsurface including simple numerical models as developed by (Hochmuth and Sunanda, 1985), ECLIPSE (Host-Madsen and Hogh Jensen, 1992), IMPES (Van Geel and Sykes, 1997), ARMOS (Waddill and Parker, 1997), and STOMP (Oostrom et al.,1997.; Oostrom et al., 2006). The two most commonly used pressure-saturation *(p-S)* functions in multiphase flow numerical simulator were developed by Brooks and Corey (1964) and van Genuchten (1980).These functions have been developed for two-phase flow. The modeling of the flow of NAPL in an unconfined aquifer requires the three phase constitutive relationship between fluid permeability, saturation and pressure (*k-S-p*) to solve the governing equations (Kechavarzi et al., 2005). Despite this need there has been a lack of data regarding these hydraulic functions, major obstacles being experimental complexity of measuring *k-S-p* functions in three phase system (Miller et al., 1998).

The overall objective of this study was to investigate the impact of layered heterogeneity on flow pattern of LNAPL in a 2-D numerical model using STOMP. STOMP is a three dimensional, multi-phase, multi-component, variable temperature, finite difference numerical simulator developed by the Pacific Northwest National Laboratory (White and Oostrom, 1996). To accomplish the objective, the following plan was implemented:

- Use STOMP to simulate a LNAPL spill in a homogeneous soil, and compare the results to an experiment conducted in a 2-D glass tank.

- To study the effect of heterogeneity on spreading behavior of LNAPL in an unsaturated zone.

CHAPTER 2

BACKGROUND

Contamination of soil and aquifer systems by non-aqueous phase liquid (NAPL) has become a widespread problem. Within past 20 years many studies on soil and ground water contamination by NAPL have been studied. Fuel spills and leaks from commercial and domestic underground storage tanks are example of LNAPL releases that occurs near the soil surface in an unconfined aquifer (Schroth et al., 1998). Improved knowledge of LNAPL movement and distribution in the subsurface is essential for risk assessment and remediation technology design. Unfortunately, the understanding of LNAPL movement, particularly in heterogeneous vadose environments, is still under investigation (Schroth et al., 1998). Several experimental studies have been reported. Qualitative experiments by (Kueper et al., 1989; Schroth et al., 1998; Wipfler et al., 2004) have provided an understanding of some multiphase processes under varied hydrogeological conditions. These experiments have been conducted to study the behavior of NAPL in the unsaturated zone. Experiments conducted by (Lenhard and Parker, 1988) have focused on developing and improving the constitutive relations commonly used in modeling of multiphase flow. Properties of multiphase systems (e.g. interfacial tension, capillary pressure, density and viscosity of each fluid phase) and porous media (e.g. porosity, pore size distribution) are important parameters in determining the extent and temporal aspects of NAPL spreading behavior in the subsurface (Das et al., 2004).

Heterogeneities in the media properties play a crucial role for defining the NAPL movement and distribution on subsurface (Miller et al., 1998). Various aspects of multiphase flow in different heterogeneity patterns over different scales of observation have been studied by large number of authors (Abriola et al., 2000; Ataie-Ashtiani et al., 2001; Duijn et al., 1995; Oostrom et al., 1999; Zhou, 2001). Experiments by (Ataie-Ashtiani et al., 2001) and theoretical studies have shown that heterogeneity on media plays a significant role on spreading behavior of NAPL in the porous medium. Understanding of the mechanisms that control NAPL behavior and the ability to predict the subsurface distribution of NAPL contribute to the success of remediation efforts (Wipfler et al., 2004).

2.1 Numerical Model Studies

A number of numerical simulators have been developed to model NAPL flow and transport in the subsurface (Abriola and Pinder, 1985; Corapcioglu and Baehr, 1987; Kaluarachchi and Parker, 1989; Kueper and Frind, 1991; Oostrom et al., 2006). These models are used as conceptual tools, and in associated with field data, they are used to describe a particular NAPL contamination problem and movement in the subsurface (Kechavarzi et al., 2005). A few one dimensional (Eckberg and Sunada, 1984; Lenhard et al., 1993; Reible et al., 1990; Thomson et al., 1992) and two dimensional quantitative experiments have been conducted to study the behavior of NAPL in the unsaturated zone (Host-Madsen and Hogh Jensen, 1992; Illangasekare et al., 1995; Oostrom et al., 2003; Pantazidou and Sitar, 1993; Van Geel and Sykes, 1994). During the past two decades, much more information has been available on laboratory and numerical simulations of NAPL. Mercer and Cohen (1990) published the review on properties, characterization and remediation of NAPL. Gelhar et al. (1992) published a critical review of

dispersivity observations from 59 different field sites, compiling variations of aquifer characteristics and dispersivity determination (S.A. Kamaruddin, 2011). Chevalier and Petersen (1999) provided an overview of NAPL flow, its transport and remedial techniques in two dimensional laboratory aquifer models. The recent collective reviews on multi-dimensional, multi-fluid, intermediate scale experiments cover experimental aspects of NAPL dissolution and enhanced remediation (Oostrom et al., 2006), in additional to flow behavior, saturation imaging and quantification (Oostrom et al., 2007). The existing LNAPL infiltration and redistribution experiments that applied numerical models include simple numerical model (Hochmuth and Sunada, 1985), ECLIPSE (Host- Madsen and Jensen, 1992), IMPES (van Geel and Sykes, 1997), ARMOS (Waddill and Parker, 1997) and STOMP (Oostrom et al., 1997; Oostrom et al., 2006; Wipfler et al., 2004). Table 2.1 is a summary of LNAPL infiltration and redistribution experiments in the unsaturated zone.

Table 2.1: Summary of LNAPL experiments in 2-D tank.

Tank size (cm^3)	Material	Media	LNAPL	Researcher
40x90x5	Plexiglass	Homogeneous	Soltron	Hochmuth and Sunada, 1985
100x100x8	Plexiglass	Homogeneous	Bayoil 82	Host-Madsen and Jensen,1992
24x24x24	Acrylic	Homogeneous	Soltron220	Simmons et al.,1990
100x167x5	Glass, kynar	Homogeneous	Soltron220	Oostrom et al.,1997
120x150x6	Glass	Homogeneous	n-heptane	Van Geel and Sykes, 1997
108x152x8.2	Ultem plastic	Homogeneous	Soltron 130	Waddill and Parker, 1997
60x50x1	Glass	Heterogeneous	Soltron 220	Schroth et al., 1998b
40x40x2.5	Plexglss	Heterogeneous	Jet fuel A-1	Wipfler et al., 2004
75x102x5.5	Glass	Homogeneous	Lard oil	Oostrom et al., 2006

2.2 Numerical Simulations

The use of numerical simulation requires a basic understanding of the theoretical formulation behind the most common codes and numerical models (S.A. Kamaruddin et al., 2011). Lewis et al. (1998) developed a numerical model that describes the flow of multiphase immiscible fluids in a deforming porous medium. The basic model or (*p-k-S*) relationship was developed without considering the effect of hysteresis. Since natural phenomena are normally affected by fluid entrapment and saturation hysteresis, ignoring the effect of hysteresis may contribute to error in simulating the natural LNAPL subsurface contamination (S.A. Kamaruddin

et al., 2011). The theoretical understanding of LNAPL movement in porous media was

developed by taking into consideration of multiphase flow formulation, mass continuity and

constitutive relationship (S.A. Kamaruddin et al., 2011). The constitutive relationships are

comprised of capillary pressure and saturation, relative permeability and saturation.

2.3 Capillary Pressure Studies

A crucial component of all multiphase flow models is the functional relationship among

relative permeability (k), fluid saturation (S), and capillary pressure (p). The theory of capillarity

was first discussed by Leverett (1941). Based on Corey (1964), the capillary pressure, P_c is

given by:

$$P_c = P_n - P_w \ = \ \frac{2\sigma \, cos\theta}{r} \tag{2.1}$$

where, P_n is the pressure in non-wetting phase, P_w is the pressure in wetting phase, σ is

the interfacial tension, θ is the contact angle and r is the effective pore radius. The effective pore

radius is dependent upon the pore size and the amount of fluid present. Wettability is related to

interface between solid and fluid, and fluid and fluid (Figure 2.1). Anderson (1987) mentioned

that the location, flow, and distribution of fluids in a porous medium are governed by wettability.
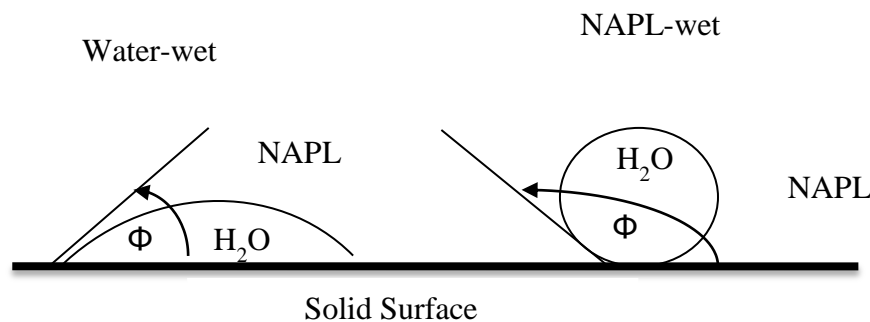
Figure 2.1: Contact angle and wetting and non-wetting interface adapted from Mercer and Cohen
(1990)

Based on the contact angle, a system can be defined as water-wet or NAPL- wet. Contact angle at the interface of a solid and a fluid or two fluids is measured by Young's equation:

$$\cos\phi = \frac{\sigma_{ns}-\sigma_{ws}}{\sigma_{nw}} \qquad (2.2)$$

where:

ϕ = contact angle

σ_{ns}= surface tension between NAPL and solid

σ_{ws}= surface tension between water and solid

σ_{nw}= surface tension between NAPL and water

When the contact angle is less than 70° the system is said to water –wet, if the contact angle is between 70° to 110° the system is said to be in the intermediary phase, if the contact angle is more than 110° the system is NAPL-wet (Mercer and Cohen, 1990).The wettability of NAPL- water system is complex and factors such as the particle size, the nature of NAPL, the chemical composition of water, the presence of surfactant affects the wettability of system (Mercer and Cohen, 1990). Brooks and Corey (1964) and van Genuchten (1980) presented one of the pioneering models describing capillary pressure- saturation relationship. The relation can be expressed using the following expression for Brooks and Corey (1964):

$$S_e= \frac{S_w-S_{rw}}{1-S_{rw}} = \left(\frac{h_d}{h_c}\right)^{\lambda} \qquad (2.3)$$

where:

S_e= effective saturation

S_w = water saturation

S_{rw}= residual water saturation

h_d = displacement pressure head

h_c = pressure head

λ = fitting parameter for the pore size index

The same relation can be expressed using the following expression for van Genuchten (1980):

$$S_e = \frac{S_w - S_{rw}}{1 - S_{rw}} = \left(\frac{1}{1 + (\alpha h_c)^n}\right)^m \qquad (2.4)$$

$$\alpha = \frac{1}{h_b}\left(2^{1/m} - 1\right)^{1-m} \qquad (2.5)$$

$$n = \frac{1}{1-m} \qquad (2.6)$$

where:

h_b = bubbling pressure

α, m, n are soil parameters.

2.4 Relative Permeability- Saturation Relationship

The relationship of *k-S* measurement experimentally is very difficult task. Numerous relationship of *k-S* has been proposed till date but most commonly used expression for *k-S* relationship is again provided by Brooks and Corey (1964) and van Genuchten (1980). For wetting phase and non- wetting phase relative permeability, van Genuchten (1980) stated:

$$k_{rw} = \bar{S}_w^{1/2}\left[1 - \left(1 - \bar{S}_w^{1/m}\right)^m\right]^2 \qquad (2.7)$$

$$k_{rn} = (1 - \bar{S}_n)^{1/2}\left[1 - \left(1 - \bar{S}_n^{1/m}\right)^m\right]^{2m} \qquad (2.8)$$

where: k_{rw} = aqueous relative permeability

  k_{rn} = NAPL relative permeability

  $\bar{S}_w$ = effective water saturation and $\bar{S}_n$ = NAPL saturation

According to Brooks and Corey (1964)

$$k_{rw} = \bar{S}_w{}^{(2+3\lambda)/\lambda} \tag{2.9}$$

$$k_{rn} = (1 - \bar{S}_n)^2 \cdot \left(1 - \bar{S}_n{}^{(2+\lambda)/\lambda}\right) \tag{2.10}$$

where: k_{rw} = aqueous relative permeability

k_{rn} = NAPL relative permeability

$\bar{S}_w$ = effective water saturation and $\bar{S}_n$ = NAPL saturation

In these equations λ is empirical coefficient related to pore size distribution and

m is a soil parameter.

The effective water saturation, $\bar{S}_w = \dfrac{S_w - S_{wr}}{1 - S_{wr}}$ \hfill (2.11)

where: S_{wr} is the residual water saturation and S_w is water saturation

In comparison to both *k-S* expressions, the Brooks and Corey have been shown to

provide, a better experimental representation for LNAPL phase (S.A. Kamaruddin et al., 2011).

This is because the Brooks and Corey model always calculates a lower *k* of LNAPL than does

the van Genuchten model, which overestimates NAPL penetration speed and distance in the

variably saturated porous medium. Both models used different pore-size distribution parameter

in the (k_r) relative permeability function derivations.

2.5 Saturation

Saturation is the fraction of the pore space that is occupied by the given fluid phase.

$$S_i = \frac{\text{Volume of the fluid}}{\text{Volume of the void space}} \tag{2.12}$$

The pore space can be filled by different fluids (air, water, or LNAPL) that are not miscible (do not mix) with each other. The fraction of the pore space that is occupied by a given fluid phase is called the saturation. The sum of the fluid saturations should total 1, or 100%.

2.6 NAPL Thickness

Various equations have been developed to predict the thickness of NAPL plume. Among these equations are Pantazidou and Sitar (1993) equation and the Schroth et al. (1995) equation.

In Pantazidou and Sitar (1993), the thickness of a NAPL plume is computed using the following equations:

$$T = \frac{1}{(\rho_o g)}\left[\frac{4(\sigma_{ow} + \sigma_{oa})}{d_n} - \rho_w g h_w\right] \qquad (2.13)$$

In Schroth et al. (1995), the thickness of a NAPL plume is computed using the following expression:

$$T = \frac{4(\sigma_{aw} - \sigma_{ao} - \sigma_{ow})}{dg(\rho_w - \rho_o)} \qquad (2.14)$$

where:

T = lens thickness or plume thickness (cm)

σ_{oa} = interfacial tension between oil and air (dynes/cm)

σ_{ow} = interfacial tension between oil and water (dynes/cm)

ρ_o = density of the oil (g/cm^3)

ρ_w = density of water (g/cm^3)

g= acceleration of gravity (cm/sec^2)

d_n= pore neck diameter (cm)

h_w = height of the lens above the water table (cm)

The pore neck (d_n) in equation 2.13 is determined by the relation (d_n) = 0.42 d_{50} (Ng et al., 1978) used for random packing

Image analysis was used to measure the plume size. The software that was used to analyze the plume size was Image J (NIH, Maryland). Image J is public domain software developed at the National Institutes of Health (NIH).This software is capable of calculating area and pixel value statistics of selected picture. It is user-friendly software, easy to draw lines and polygons, easy to measure distance and angles on a given picture. The spatial calibration tools help physical dimensional measurements in different units as centimeters or inches. The Image J software was also used to compare the thickness of plume with that of experiment plume thickness.

2.7 Numerical Model and its Application

Many numerical models are available for NAPL simulations. These models are capable of simulating multidimensional analysis based on finite difference or finite element methods. Some of the available numerical modes performing multidimensional analysis based on finite difference are UTCHEM, TOUGH2, and STOMP. Common finite element models are MOFAT, NAPL simulator (S.A. Kamaruddin et al., 2011). A summary of existing 2-D numerical models designed for NAPL simulations are presented here in Table 2.2

Table 2.2: Existing 2-D numerical models designed for NAPL simulations

Numerical model	Description of model	Method	Reference
ARMOS	Areal multiphase organic simulator program	Finite element	(Kaluarachchi and Parker 1990)
MAGNAS	A multidimensional finite element transport of water, NAPL and air through porous media	Finite element	Huyakorn et al. 1992
MOFAT	A 2-D finite element program for multiphase flow and transport	Finite element	Katyal et al., 1991
NAPL Simulator	A 2-D model for movement and fate of NAPL contaminants in near surface granular soils	Finite element	Guarnaccia et al., 1997
STOMP	Subsurface transport over multiphase phase model	Finite difference	Oostrom et al., 2007
TOUGH2v2	A simulator for non-isothermal flows of multi-component, multiphase fluids	Finite difference	Pruess et al., 1991
UTCHEM	A 3-D chemical flood simulator	Finite difference	Center for Petroleum and Geo system Engineering (2000)
VENT2D	A multi-component vapor transport and phase distribution model	Finite difference	Benson (1994)

CHAPTER 3

MODEL DESCRIPTION

This chapter presents an overview of STOMP and input files/output files of the model

used for the thesis. Additional information of numerical simulator STOMP can be found in the

user manual provided by White and Oostrom (1996).

3.1 Model Description

The numerical simulator Subsurface Transport Over Multiple Phases (STOMP) (White

and Oostrom, 1996) was chosen for our simulation work in this research work. The STOMP

simulator has been developed by the Pacific Northwest National Laboratory for the modeling of

subsurface flow and transport systems and remediation technologies (White and Oostrom, 1996).

STOMP is a three dimensional, multiphase, multi-component, variable temperature, finite

difference numerical simulator. STOMP can model problems with parameters like dispersion,

diffusion, dilution effects, interfacial tension, relative permeability, capillary pressure, capillary

trapping, phase density, liquid saturation and other minor factors. STOMP allows the use of a

well to inject contaminant, surfactant and water and also additional well for recovery of

contaminant. The STOMP simulator is designed with a variable source code, where source code

configurations are referred to as operational modes. Operational modes are classified according

to the solved governing flow and transport equations (White and Oostrom, 1996). The mentioned

capabilities make STOMP one of the most comprehensive model available for modeling of

contaminant transport.

STOMP has been used fairly widely in the past and has been successfully validated and

applied to simulate a variety of multi-phase problems (e.g. Schroth et al., 1998; White and

Oostrom, 1996; Oostrom et al., 1999; Ataie-Ashtiani et al., 2001). STOMP is mainly composed

of a series of FORTRAN subroutines to solve the governing differential equations. STOMP recommends the use of MS Excel©, Surfer©, Tecplot© and Gnuplot© for post processing of output files. Detail of input files and procedure for using STOMP is included in Appendix (Appendix A: Input files and Appendix B: Instruction).

3.2 Simulation Description

The simulation performed in this research used the nonhysteretic two-phase version of the water- oil mode (w-o) of STOMP. The governing conservation equations are discretized to algebraic form following the integrated- finite- difference method of Patanaker (1980).

Conservation of Mass

The following section summarizes Ataie-Ashtiani et al. (2001). The balance equations for STOMP in the water-oil mode are (1) the mass balance equation (2) pressure equation. The following mass balance equation for the phases water (*w*) and oil (*o*) are:

$$\frac{\partial}{\partial t}(\eta \rho_i S_i) = -\nabla \cdot (\rho_i q_i) \quad \text{for } i = w, o \tag{3.1}$$

where:

$$q_i = -\frac{k_{ri}k}{\mu_i} \cdot (\nabla P_i + \rho_i g e_g) \quad \text{for } i = w, o \tag{3.2}$$

In these equation subscripts *i* may be *w* for the water phase or *o* for the nonaqueous (oil) phase, η is a porosity, ρ is density (ML^{-3}), S is a saturation, q is fluid flow velocity (LT^{-1}), k_r is relative permeability, k is intrinsic permeability (L^2), μ is a viscosity $(ML^{-1}T^{-1})$, P is pressure $(ML^{-1}T^{-2})$, g is the magnitude of gravitational acceleration (LT^{-2}), and e_g is the unit vector in vertical direction.

In additional to the well- known van Genucthen (1980) and Brooks and Corey (1964) capillary pressure-saturation relations, this version of STOMP also allows for tabular input of fluid saturations and pressures. In our numerical simulation in this thesis, the Brooks- Corey formula for capillary pressure was used.

$$S_e = (P_c/P_d)^{-\lambda} \text{ for } P_c \geq P_d \tag{3.3}$$

where:

$$S_e = \left(\frac{S - S_e}{1 - S_r} \right), 0 \leq S_e \leq 1 \tag{3.4}$$

In these equations, P_c is a capillary pressure, P_d is displacement pressure, S_e is effective saturation, S_r is irreducible water saturation, and λ is the pore size distribution index. The relative permeability of the medium to the aqueous phase, k_{rw} and nonaqueous phase, k_{rn}, are given by Brooks- Corey- Burdine formula (Brooks and Corey, 1964).

$$k_{rw} = S_e^{[(2+3\lambda)/\lambda)]} \tag{3.5}$$

$$k_{rn} = (1 - S_e)^2 \left(1 - S_e^{[(2+\lambda)/\lambda)]} \right) \tag{3.6}$$

The set of equations was solved with a multivariable, residual-based Newton- Raphson iteration technique. The constitutive relations were computed numerically (White and Oostrom, 1997). The computation domain was discretized using a constant nodal spacing of 0.3 cm in both horizontal and vertical directions. A time step of 1 min was used throughout the simulation. The

maximum number of Newton iteration was 32, with a convergence factor of 10^{-6}. Upwind interfacial averaging was used for LNAPL and water relative permeability, whereas harmonic averaging was used for the other components.

3.3 Model Output

STOMP generates a series of output data files which can be processed using MS Excel$^©$, and graphical software such as Surfer$^©$ and Tecplot$^©$. STOMP recommends uses of MS Excel$^©$ for 1-D models, Surfer$^©$ for 2-D models and Tecplot$^©$ for 2-D and 3-D models. Tecplot$^©$ was used for our output processing of simulation. Some of the major STOMP output data of the component modeled are: phase saturation, relative permeability, interfacial tension, phase pressure.

CHAPTER 4

MODEL INPUT AND OUTPUT

The STOMP simulator is controlled through a text file, which must be titled input for proper execution. This input file has a structured format composed of cards, which contain associated groups of input data. In this research, two fluid phases of water and oil has been simulated apart from the solid soil phase. The following are the categorical description of input parameters used in STOMP during the simulation of LNAPL movement in the an unconfined aquifer cited from the user's manual, Subsurface Transport Over Multiple Phases Theory Guide (White and Oostrom, 1996).

4.1 Model Grid

STOMP allows both two dimensional and three dimensional spatial grids with constant or variable grid block sizes. A two dimensional Cartesian coordinate system was used to establish the model domain of a 2-D tank experiment conducted by Saint Aime (2011). The 90cm x 90cm x 5cm tank was divided into a model grid consisting of 30 gridblocks in x- direction and 30 gridblocks in z-direction making the domain as 2-D aquifer. The x -and z- direction gridblocks were 3 x 3 cm^2 and y-direction has a constant gridblock of 5cm. Figure 4.1 shows the 2-D domain and grid of the modeled aquifer.
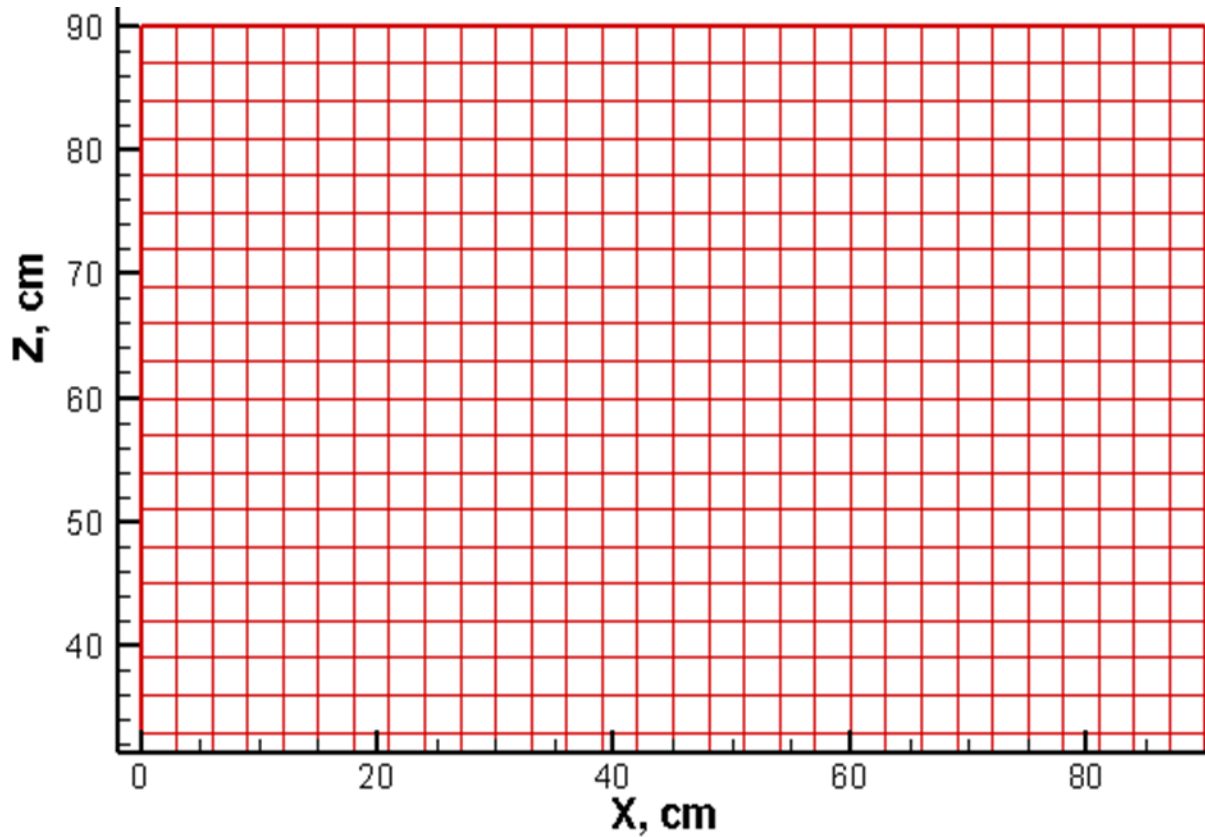
Figure 4.1: 2-D domain model grid of the modeled aquifer

4.2 Simulation Time Step

A constant time step or an automatic time step which is dependent on relative changes of component properties can be used in STOMP to discretize the total time step. The time steps can be generated in the form of days, hours or minutes. For simulation conditions which use automatic time step option, maximum and minimum time step values along with the initial time step value in the units of hours or days must be generated. If the generated or entered value slightly differs from the recommended values the model output becomes unstable and may not be able to produce any results.

4.3 Reservoir/aquifer properties for homogeneous soil system

Permeability, porosity, density and saturation are input soil parameters for STOMP. STOMP allows for constant, layer specific, or grid block specific value for porosity and permeability for true representation or reservoir properties. Table 4.1 lists the major reservoir properties adapted from Saint Aime (2011) for our numerical simulation for homogeneous soil system. A constant porosity of 0.24 has been used for entire simulation.

Table 4.1: Soil properties adapted from Saint Aime (2011)

Bulk density, ρ (g/cm^3)	1.65
Porosity (η)	0.24
Permeability, k (cm^2)	1.93 x 10^{-7}
Brooks and Corey (λ)	1
Displacement head (h_c) cm	7.67
Residual water, (S_{rw})	0.3

Permeability

The value of intrinsic permeability, k has been derived for water at 20° C (kinematic viscosity, $v = 1\text{x}10^{-6} m^2$/s) and by using the hydraulic conductivity, K value reported by Saint Aime (2011) as follows:

$$k = {}^{Kv}\!/_{g} = 1.9 \text{ x } 10^{-4} \text{ (m/s) x } 10^{-6} \ (m^2\text{/s)/ } 9.81 \ (m/s^2) = 1.93 \text{ x } 10^{-11} \ m^2$$

The study used an isotropic aquifer. A provision for modeling anisotropic aquifer has also been included in the STOMP software allowing the user to specify different permeability values for each coordinate direction. Figure 4.2 shows schematic drawing of domain setup for simulation of homogeneous soil system.
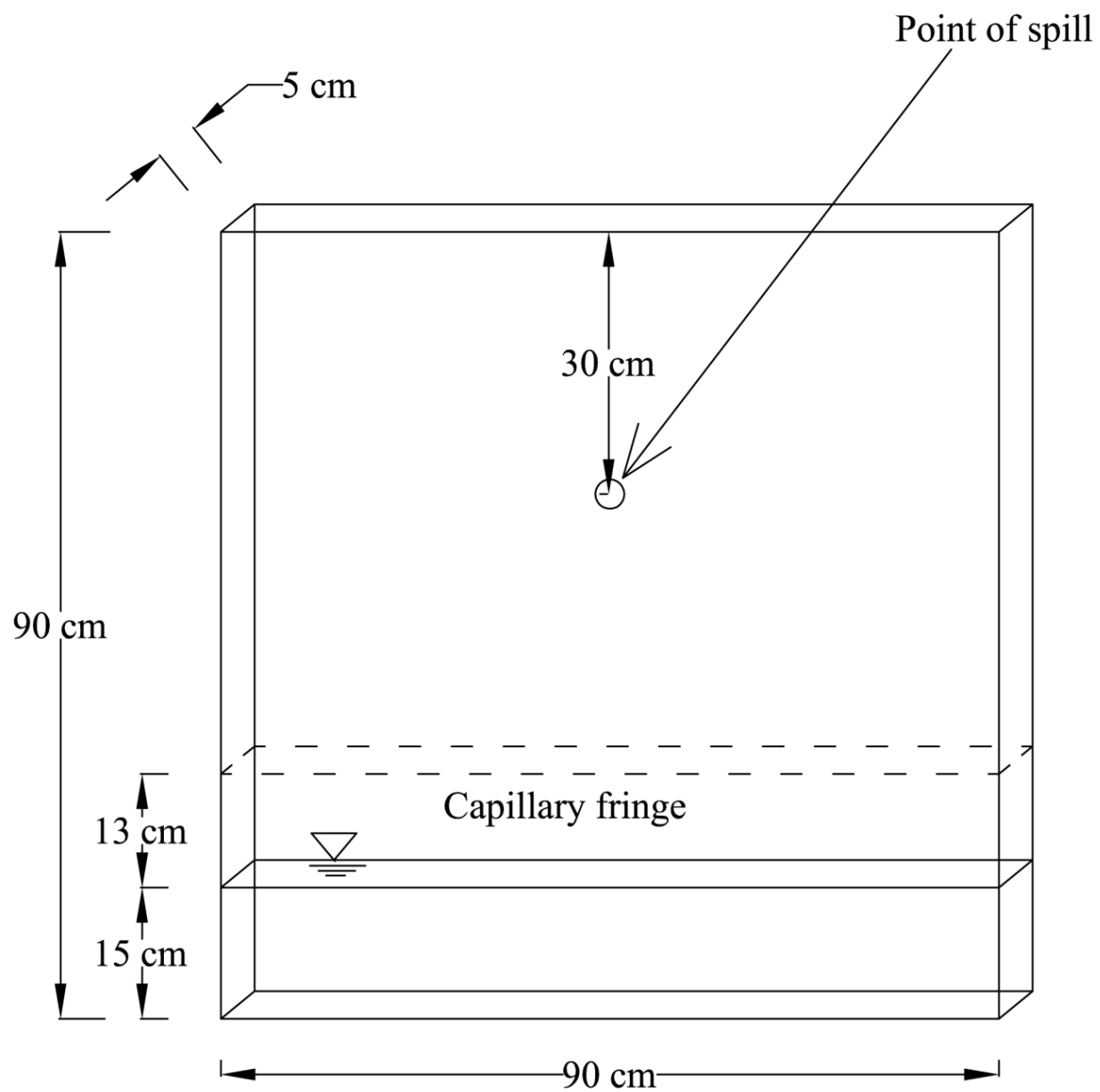
Figure 4.2: Schematic drawing of domain setup for Simulation of homogeneous soil system

4.4 Reservoir/aquifer properties for soil heterogeneous patterns

Figures 4.3 and 4.4 show the two different patterns of heterogeneity used for simulation of LNAPL movement in an unconfined aquifer for this research. The media is composed of two different sand types: coarse sand and fine sand. Properties of the sand samples adapted from Oostrom et al. (1999) are presented in the Table.4.2.

Table 4.2: Sand medium properties adopted from Oostrom et al. (1999).

Porous medium properties	Coarse sand (CS)	Fine sand (FS)
Brooks-Corey entry head, h_d (cm)	2.3	19.7
Brooks- Corey Coefficient (λ)	4.3	5.1
Water saturation(S_{rw})	0.11	0.14
Permeability, k (10^{-6}) cm^2	1.21	0.021
Porosity(η)	0.34	0.41
Density (g /cm^{-3})	1.749	1.564
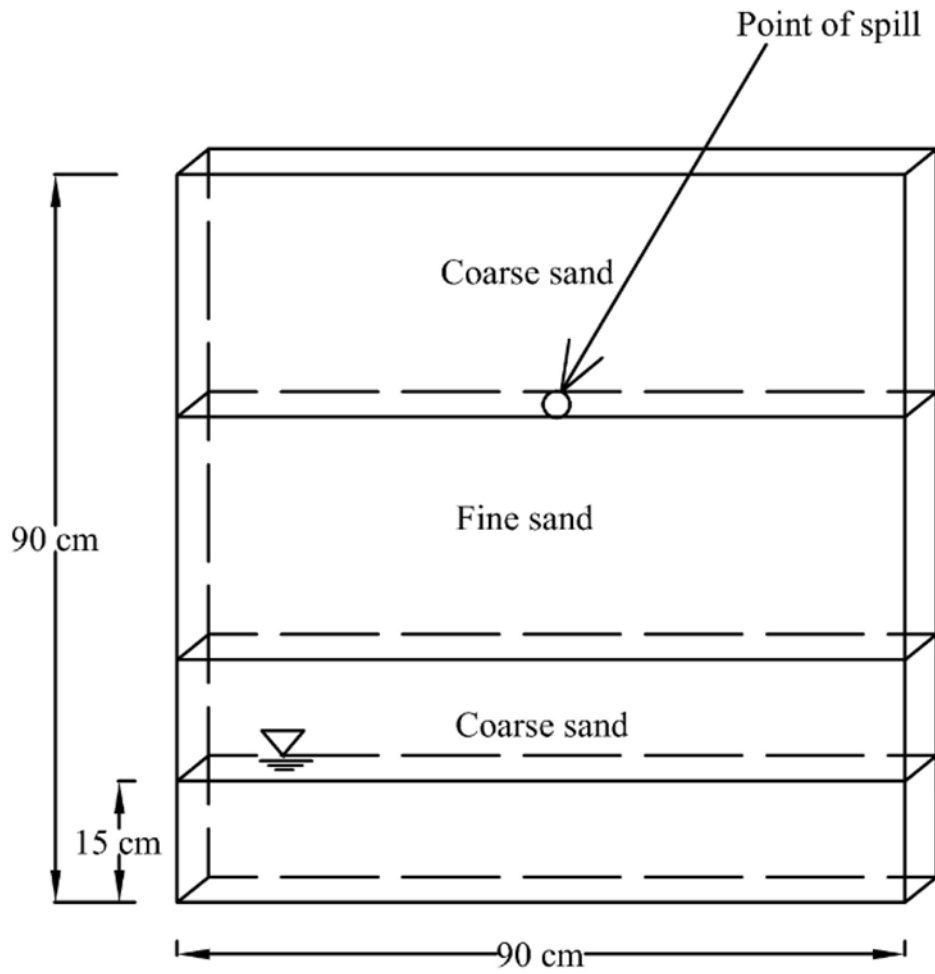
Figure 4.3: Schematic drawing of domain setup for simulation of heterogeneous soil pattern (P1)
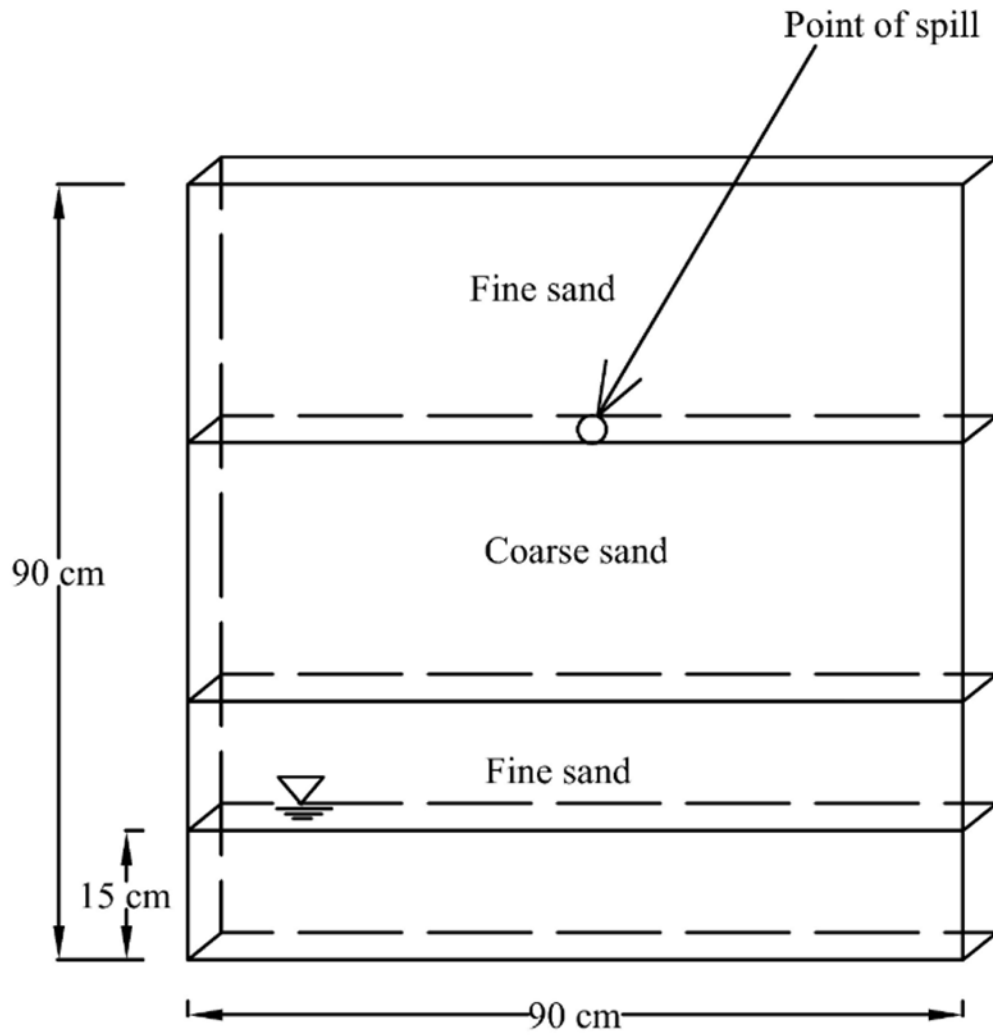
Figure 4.4: Schematic drawing of domain setup for simulation of heterogeneous soil pattern (P2)

4.5 Initial Conditions

Pressure and water saturation of the aquifer were used for the initial condition of the simulation. A constant value of initial pressure which is equal to the atmospheric pressure within an unconfined aquifer, and a hydrostatically varying initial pressure below the water table line was used for the simulations. No initial saturation options are allowed for the three-phase, aqueous-NAPL-gas, operational modes (e.g., STOMP-w-o (water-oil), STOMP-w-o-a (water-oil- air). For all operational modes, default values for initial conditions have been specified within STOPM as shown in Table 4.3

Table 4.3: STOMP Initial Conditions Default values (White and Oostrom, 1996)

Initial Field Variable	Symbol	Default Value
Temperatures	T	20.D+0
Pressure of phase i	P_i	101325.D+0
Saturation of phase i	S_i	0.D+0
Mole fraction of component i in phase j	$x_j{}^i$	0.D+0
Solute concentration in phase i	C_i	0.D+0
Salt concentration in phase i	S_i	0.D+0

4.6 Fluid properties

Modeling of multiphase subsurface contaminant transport requires data on the properties of the

various fluids involved including viscosity, density and fluid compressibility. Table 4.4 lists the

general fluid properties of dodecane, the LNAPL used in this study.

Table 4.4: Fluid Properties (Reid et al., 1987)

Molecular weight of dodecane	170.340 g/mol
Density of dodecane	750 kg/m^3
Density of water	1000 kg/m^3
Viscosity of dodecane	0.00134 pa s
Critical compressibility factor of dodecane	0.24
Critical pressure of dodecane	18.2 bar
Boiling point Temperature of dodecane	489.5 K
Freezing point Temperature of dodecane	263.6 K

4.7 Boundary Conditions

Boundary conditions were setup as per the physical model of the experimental tank. On

top of the model a constant atmospheric pressure were applied. The aquifer study modeled a

water table 15 cm above the bottom of the aquifer for both homogeneous and heterogeneous

studies. Two vertical sides where the drainage wells are located were sealed therefore, no liquid

flow will occur across these boundaries. Along the bottom of the model and along the two

vertical sides of the model, a constant water pressure was established due to the fixed position of

water table. The water table was used as a datum. A schematic drawing of the boundary

condition used for simulation of both homogeneous and heterogeneous soil system is shown in

Figure 4.5.
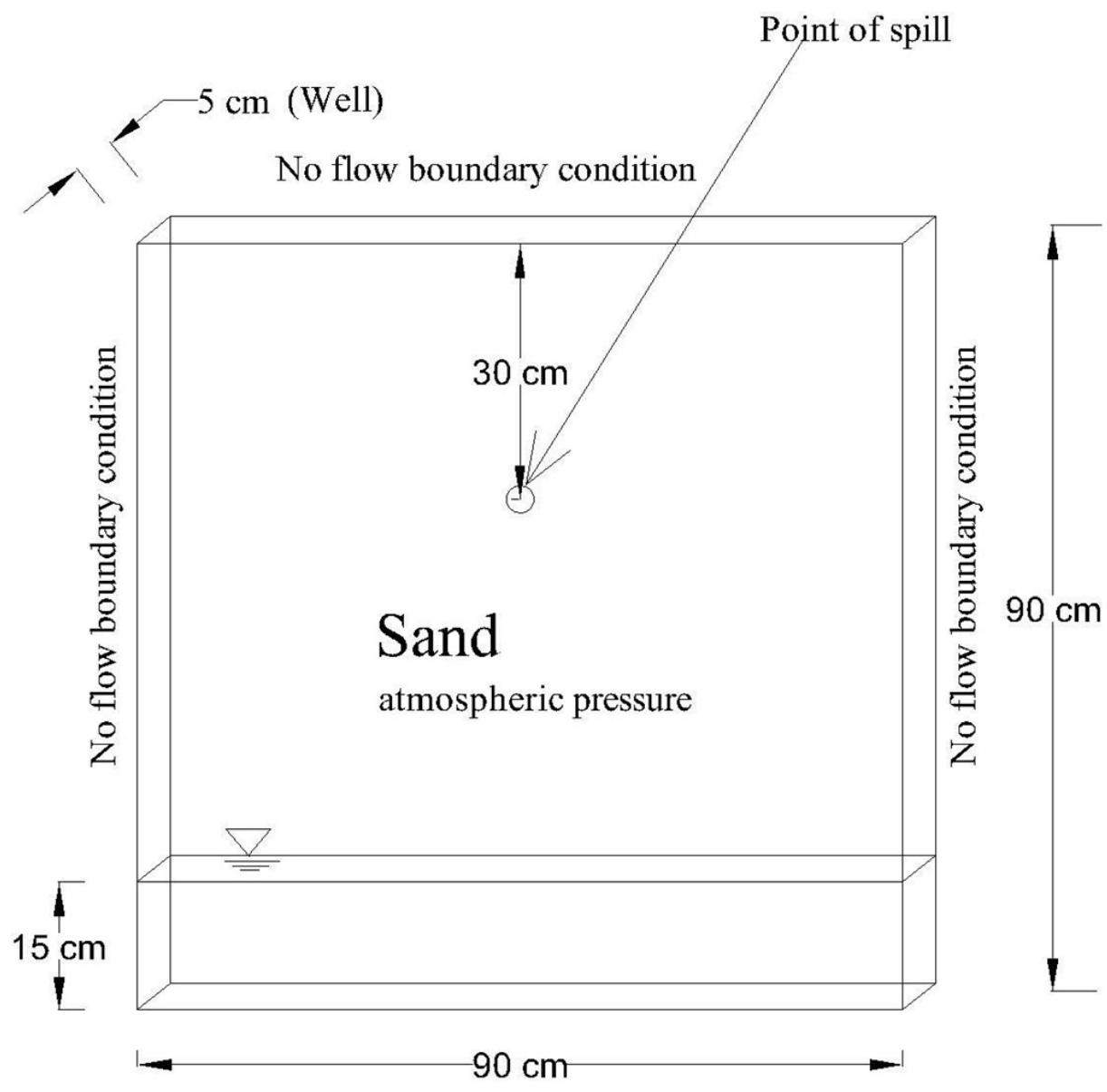
Figure 4.5: Schematic drawing of boundary condition used for simulation of both homogeneous
and heterogeneous studies

CHAPTER 5

RESULTS AND DISCUSSIONS

5.1 Numerical Simulation of LNAPL movement in a homogeneous soil using STOMP

The initial study focused on using STOMP to model 2-D experiments conducted by Saint

Aime (2011). The study was conducted in a 90cm x 90cm x 5cm glass tank. The experiments

investigated a spill of 286 ml of dodecane injected at the rate of 0.5 ml/s in homogeneous coarse

sand. The dodecane was released 30 cm below the top surface in the center of the tank. A

constant water table of 15 cm and capillary fringe of 13 cm was used for the numerical modeling.

The simulation performed in this research used the nonhysteretic two-phase version of the water-

oil mode (w-o) of STOMP.

The STOMP model was used to simulate the spill for 5 hour (Figure 5.1- 5.3). After 30

minutes the model indicated that the LNAPL spread into an oval-shaped pool. After 1 hour,

gravitational flow became dominant. As a result, rate of horizontal migration due to capillary

forces became small compared to the rate of vertical movement. Capillary forces are holding the

water in the capillary fringe while buoyancy forces are keeping the NAPL above the water. Since

LNAPL is less dense than water LNAPL started accumulating just above the capillary fringe

region (Figure 5.1).

The LNAPL reached the top of capillary fringe with maximum LNAPL saturation of

approximately 0.22, as indicated by the yellow color of oil saturated region in figure 5.1. After 2

hours, the LNAPL accumulated on the top of the capillary fringe started moving horizontally.

During this redistribution (3 hours to 5 hours after the spill), the LNAPL saturation started decreases to a constant saturation value of approximately 0.2 (Figure 5.2- 5.3). Detail of input files is in Appendix A.
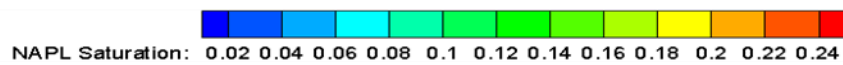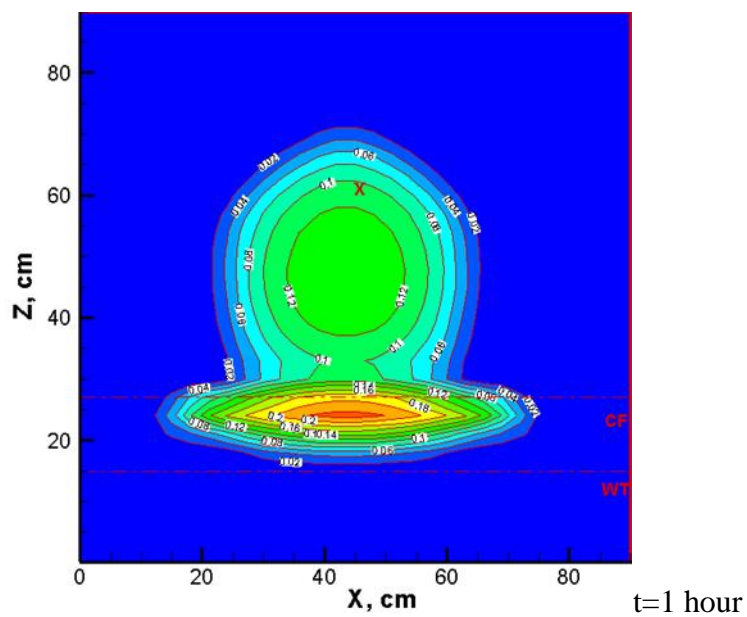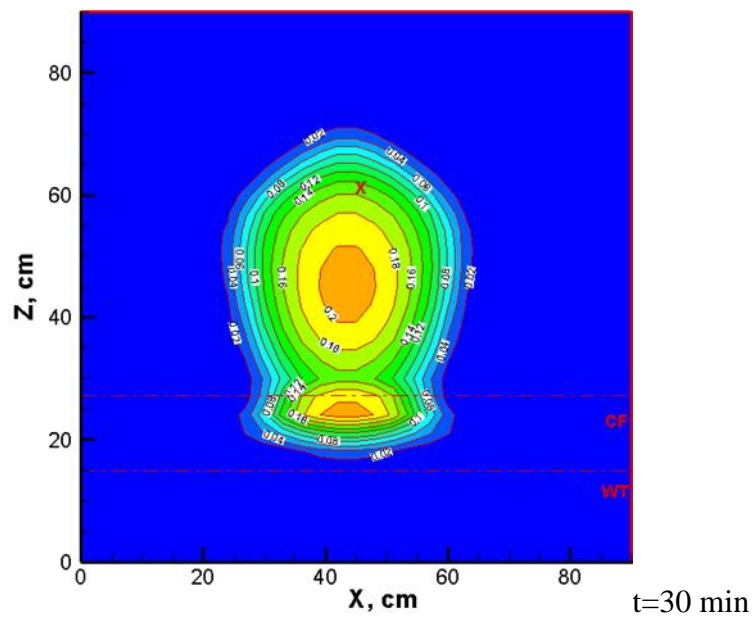
Figure 5.1: Simulation of LNAPL movement at t= 30 min and t= 1hour showing release point, x=30 cm from top, water table, WT=15 cm, capillary fringe, CF=13 cm, saturation, S= 0.02-0.22
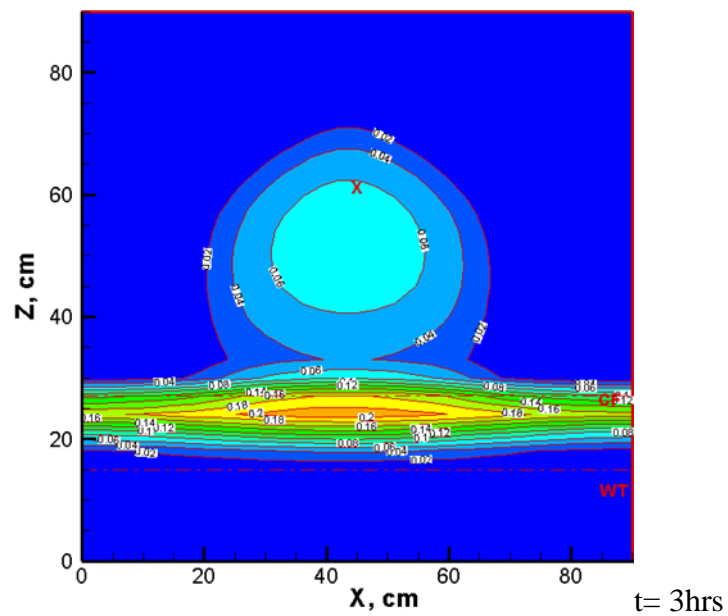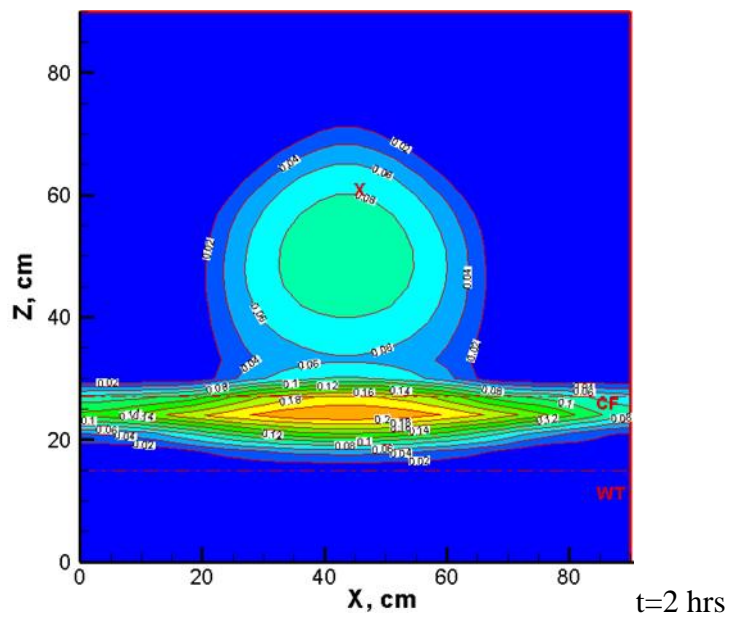
t=2 hrs

t= 3hrs

Figure 5.2: Simulation of LNAPL movement at t= 2 hrs and t= 3 hrs with saturation, S= 0.12-0.2
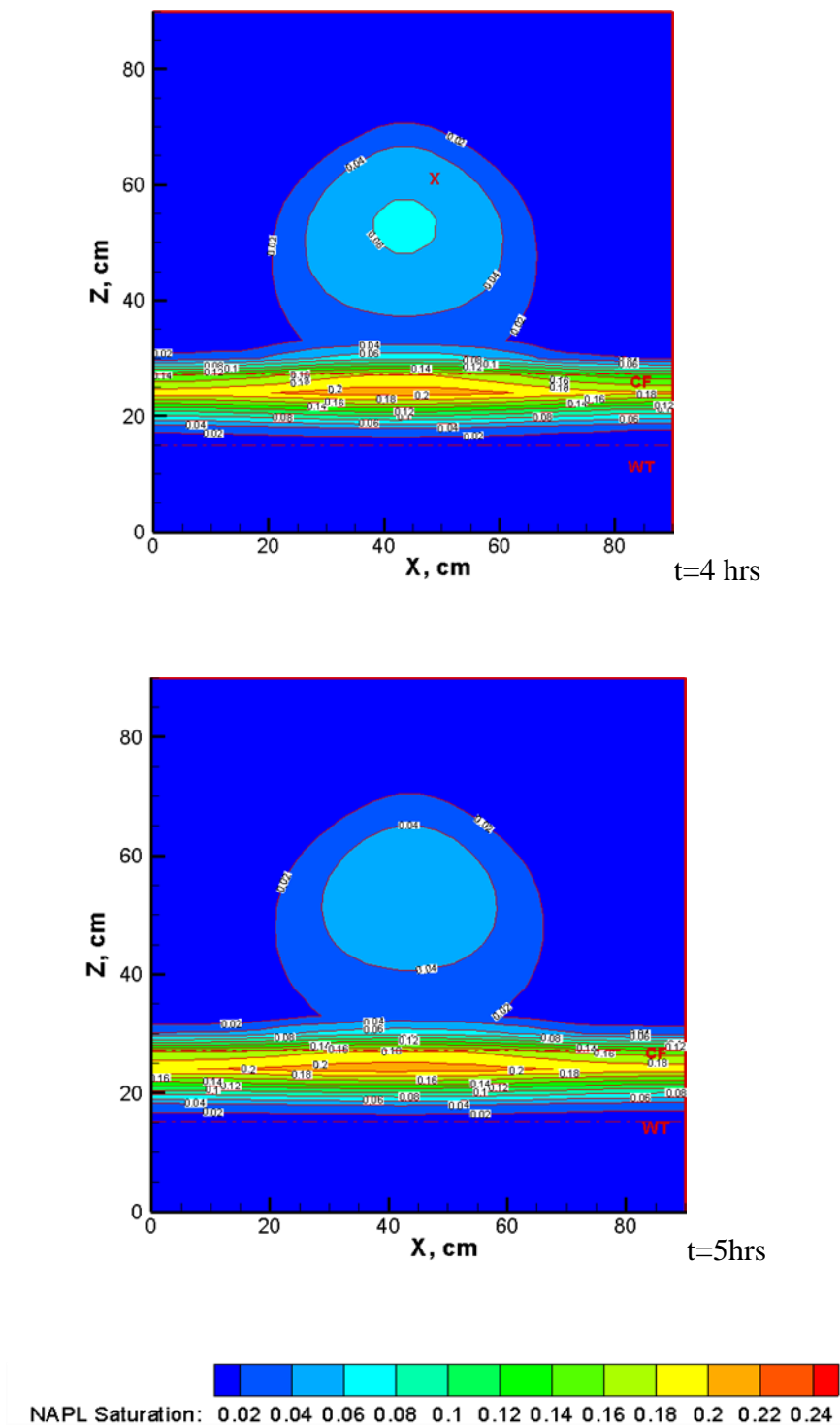
t=4 hrs

t=5hrs

Figure 5.3: Simulation of LNAPL movement at t= 4 hrs and t= 5 hrs with saturation, S= 0.18-0.2

5.2 Comparison of numerical simulation to 2-D experiment

The results of numerical simulation were compared with the experimental results performed in the laboratory of Southern Illinois University by Saint Aime (2011). In this experiment, a constant water table of 15 cm was maintained using a carboy to maintain a constant head. The d_{50} of Ottawa sand was reported as 0.6 mm, resulting 13 cm capillary fringe in the simulation tank. Additional soil properties and sand parameter from pressure saturation experiment used for the Brooks and Corey expression are presented in table 5.1

Table 5.1: Property of the sand

Bulk density, ρ (g/cm^3)	1.65
Porosity, (η)	0.24
Specific gravity, G_s	2.64
Permeability, k (cm^2)	1.93 x 10^{-7}
Displacement head, h_d (cm)	7.67
Residual water, S_{rw}	0.3
Experimental coefficient, λ	1

The dodecane was released 30 cm below the top surface in the center of the tank. After the release of dodecane, the LNAPL infiltrated downwards from the point of spill. After 30 min all the LNAPL reached an unconfined aquifer in both the experiment (Figure 5.4a) and modeling (Figure 5.4b). After one hour, all the LNAPL from an unconfined aquifer reached the top of capillary fringe through vertical movement in both the experiment (Figure 5.5a) and modeling (Figure 5.5b). In the simulation, the maximum saturation of LNAPL occurred after one hour of release just at the top of capillary fringe. Between t= 1 hr to t= 2 hr in both experiment (Figure 5.6a) and modeling (Figure 5.6b), LNAPL started to accumulate above the capillary fringe. Because of the larger density and viscosity of water compared to air, the vertical displacement of water becomes slower as a result, the LNAPL starts to accumulate above the capillary fringe (Kechavarzi et al., 2005). As additional LNAPL accumulates above the capillary zone, an oil table will develop. Once the LNAPL reached the top of the capillary fringe they starts spreading out in the upper part of capillary fringe which can be seen in both experiment (Figure 5.7a- 5.8a) and modeling (Figure 5.7b-5.8b). After t= 5 hr, in experimental tank (Figure 5.9a) the LNAPL was seen moving horizontally toward the both ends of tank where two wells were constructed. However, the LNAPL did not reach the well, whereas in the simulation tank (Figure 5.9b) the horizontal movement of LNAPL was seen moving more towards the side wells. This difference in later spreading is an interesting point to be further investigated. Sensitivity analysis of properties of NAPL and sand media like temperature, capillary pressure, permeability, pore size distribution may further be needed to investigate for this difference in lateral spreading which was not investigated in this thesis. A comparison of the model and the experiment is shown in (Figure 5.4 - 5.9).
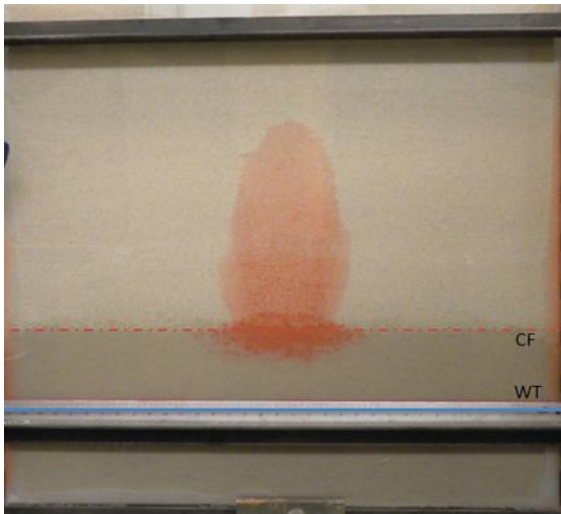
(a) Experiment (b) Modeling
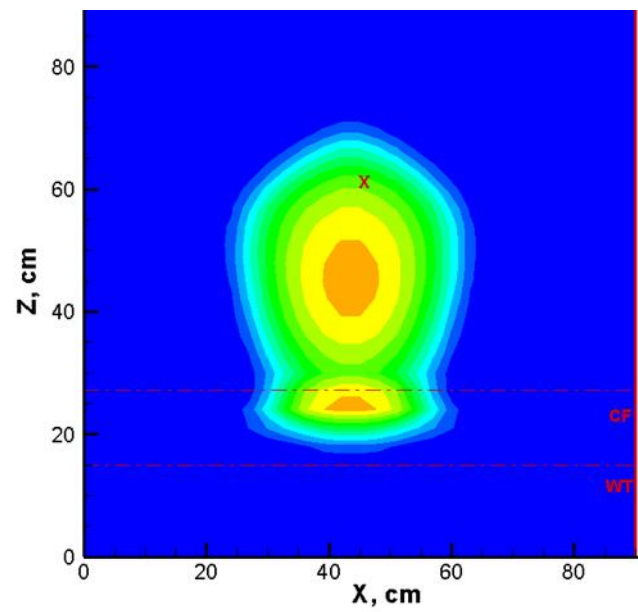
Figure 5.4: LNAPL movement in (a) experimental and (b) simulation tank at time t=30 min with x= point of release 30 cm from top, water table,WT= 15 cm, capillary fringe, CF= 13 cm

(a) Experiment   (b) Modeling
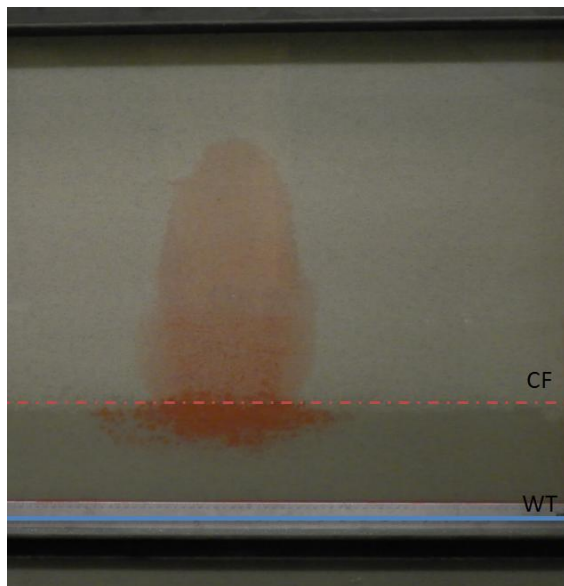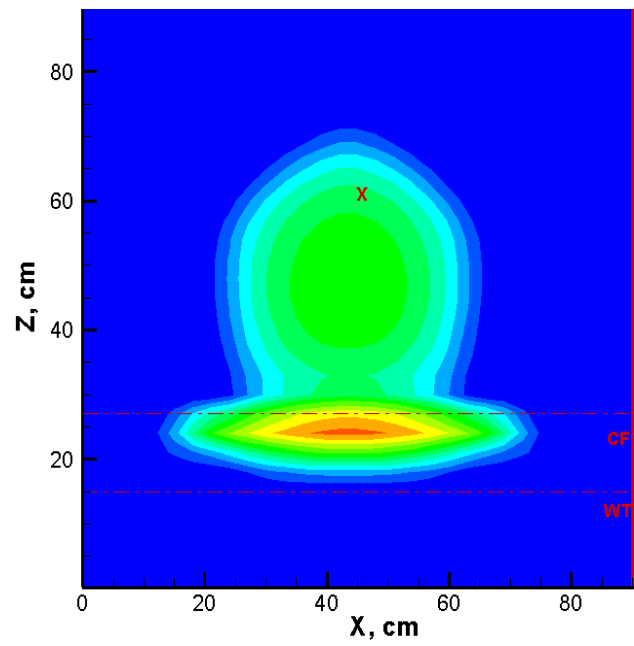
          t= 1 hour   t= 1 hour

Figure 5.5: LNAPL movement in (a) experimental and (b) simulation tank at time t= 1 hour
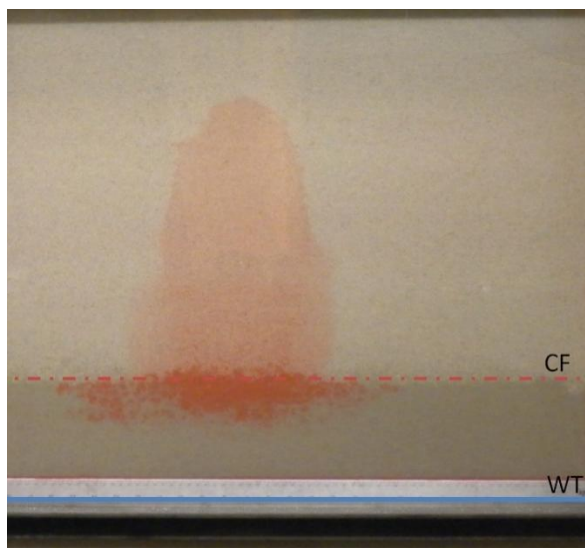
(a) Experiment (b) Modeling
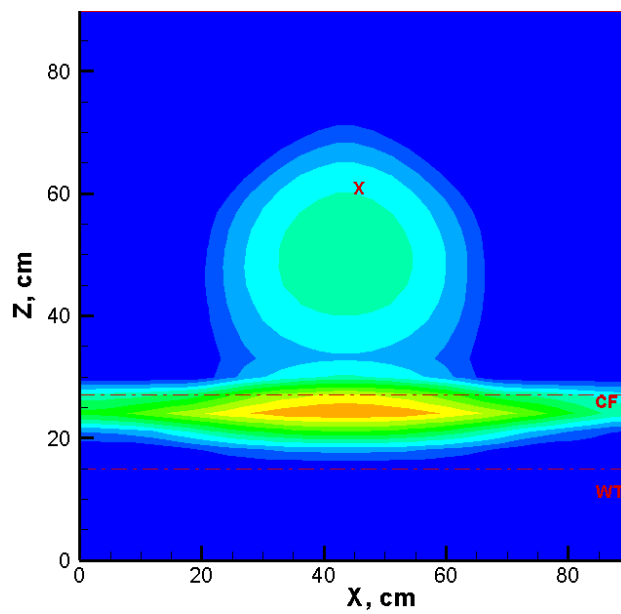
t= 2 hours t= 2 hours

Figure 5.6: LNAPL movement in (a) experimental and (b) simulation tank at time t= 2 hours

(a) Experiment
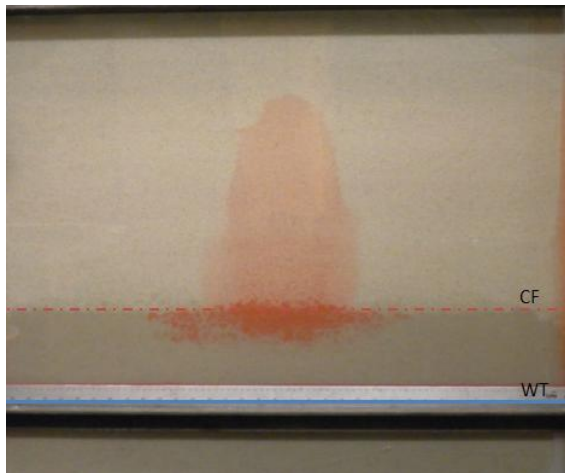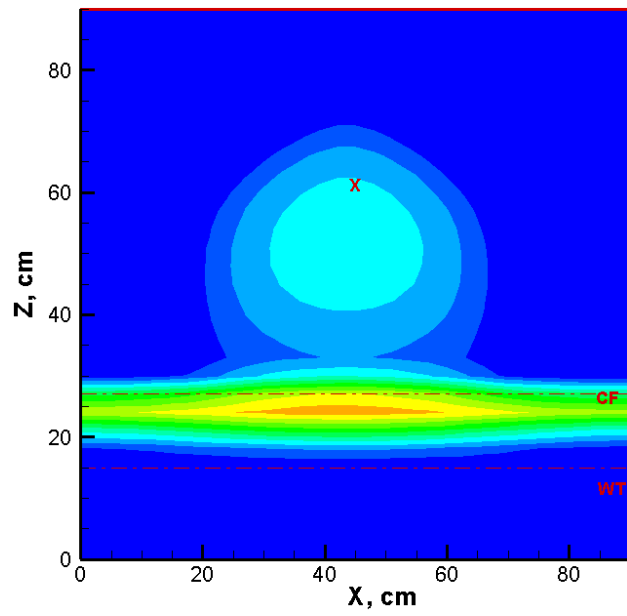
(b) Modeling

t= 3 hours

t= 3 hours

Figure 5.7: LNAPL movement in (a) experimental and (b) simulation tank at time t= 3 hours
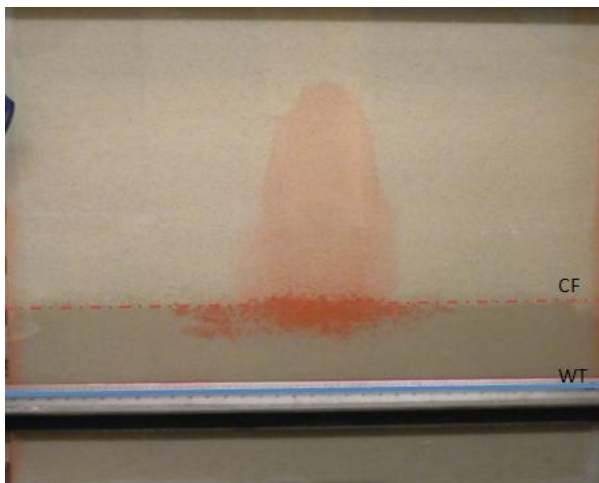
(a) Experiment   (b) Modeling
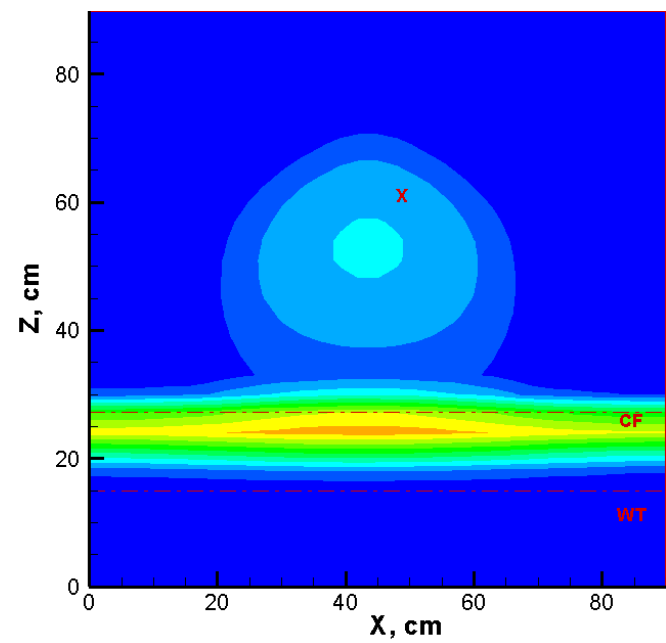
t= 4 hours   t = 4 hours

Figure 5.8: LNAPL movement in (a) experimental and (b) simulation tank at time t= 4 hours
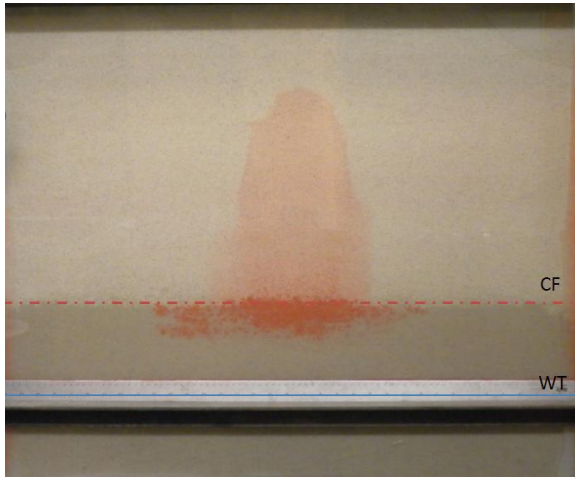
(a) Experiment   (b) Modeling
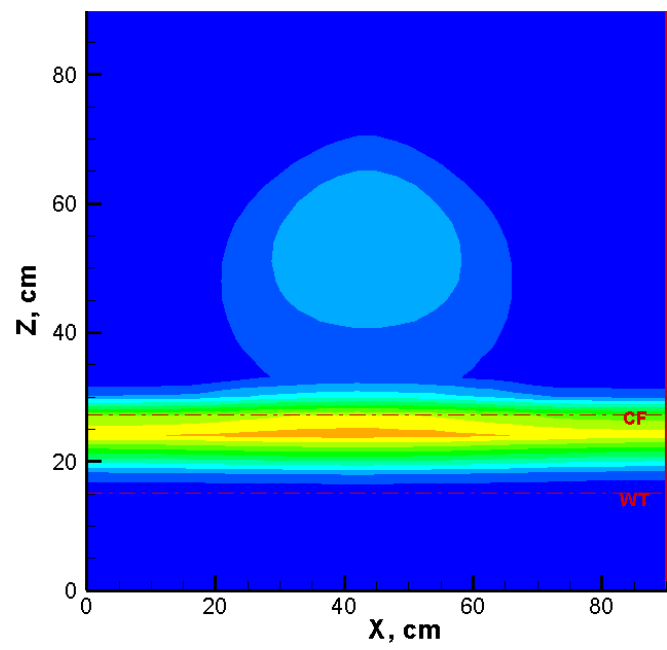
t= 5 hours   t= 5 hours

Figure 5.9: LNAPL movement in (a) experimental and (b) simulation tank at time t= 5 hours

The overall agreement between experimental and simulated results was fairly good, although some differences were observed. After t= 4 hours, the LNAPL movement was almost constant for the experimental tank (Figure 5.8a), but still some LNAPL were noticed moving towards the well in simulation tank (Figure 5.8b). Furthermore, the lateral spreading of the LNAPL was greater in terms of distance for the simulation (Figure 5.9b) than for the experiment (Figure 5.9a).

5.3 Characteristics of the plume in the simulation model

Various equations have been developed to predict the thickness of NAPL plume. Among these equations are Pantazidou and Sitar (1993) equation, Schroth et al. (1995) equation.

In Pantazidou and Sitar (1993), the thickness of a NAPL plume is computed using the following equations:

$$T = \frac{1}{(\rho_o g)}\left[\frac{4(\sigma_{ow} + \sigma_{oa})}{d_n} - \rho_w g h_w\right] \qquad (5.1)$$

In Schroth et al. (1995), the thickness of a NAPL plume is computed using the following expression:

$$T = \frac{4(\sigma_{aw} - \sigma_{ao} - \sigma_{ow})}{dg(\rho_w - \rho_o)} \qquad (5.2)$$

where:

T = lens thickness or plume thickness (cm)

σ_{oa} = interfacial tension between oil and air (dynes/cm)

σ_{ow} = interfacial tension between oil and water (dynes/cm)

ρ_o = density of the oil (g/cm^3)

ρ_w = density of water (g/cm^3)

g = acceleration of gravity (cm/sec^2)

d_n = pore neck diameter (cm)

h_w = height of the lens above the water table (cm)

The pore neck (d_n) in equation 2.7 is determined by the relation (d_n) = 0.4 d_{50} (Ng et al., 1978) used for random packing.

The length, thickness and area of the plumes were calculated using image analysis software ImageJ (National Institute of Health, Maryland), and then Pantazidou and Sitar (1993) equation was used to compare the calculated plume thickness with that of experiment conducted by Saint Aime (2011). For the comparison of plume thickness between model and experiment, the final plume at 5 hours was considered. The length, the area and the thickness of the plume at 5 hours are presented in Table 5.3. In Figure 5.6, it can been seen that at 5 hours the plume in the simulation model was located about 8.1 cm above the water table and was 57 cm long, 2.5 cm thick, and had an area of 64 cm^2. The calculated thickness of the plume in the simulation model was 4.8 cm which was found from the computed value of the thickness from equation (5.1).

Table 5.2: Plume dimension in simulation model at 5 hours using ImageJ (National Institute of Health, Maryland)

Time period	Length(cm)	Area (cm^2)
5 hr	57 cm	64 cm^2

Table 5.3: Measures and calculated thickness of the plume

Time period	Measured thickness T (cm)	Calculated thickness T' (cm)	Ratio (T/T')	Percent Difference %
5 hr	2.5 cm	4.8 cm	0.52	-48

Since the LNAPL movement towards the side wells in experiment in terms of distance travelled were less compared to simulation, the lateral spreading of the LNAPL was greater for simulation than for experiment. This percent difference of -48% might indicate that in the experiment the LNAPL lateral movement towards the side well was slow as compared to simulation, because the LNAPL may be retained in the sand as a result of high capillary forces in experiment than in simulation. Apart from this, the sensitivity of Image J software in calculating area and pixel value statistics of digital picture may not be accurate for calculating the numerical model output picture obtained from Tecplot.
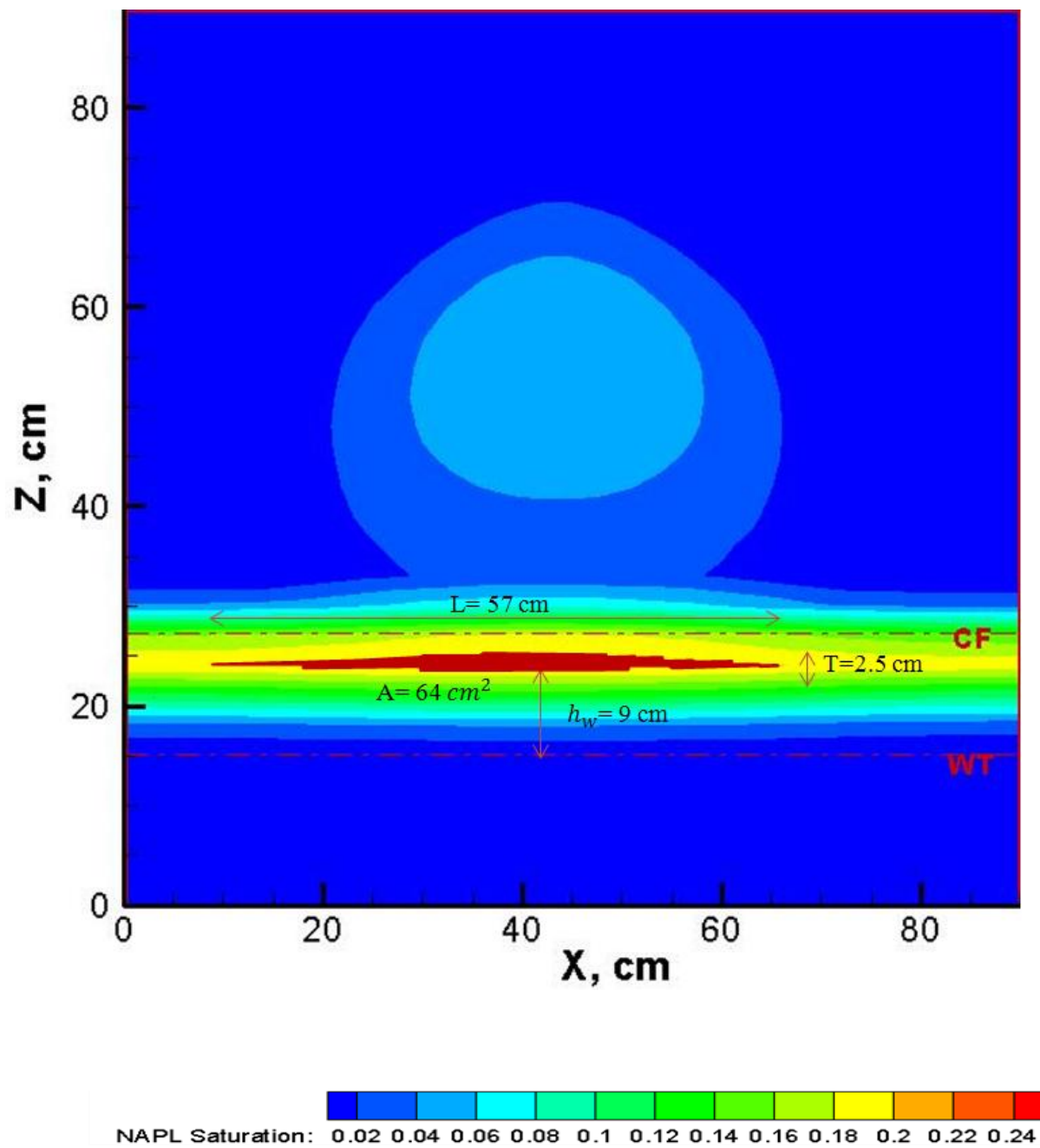
Figure 5.10: Plume in the simulation model at 5 hour

5.4 Numerical simulation of LNAPL movement in a layered heterogeneous system

Simulations were performed to evaluate the effects of heterogeneity. Two different sand types, denoted by CS for coarse sand and FS for fine sand were used. The properties of sand used for the study are presented in Table 5.5. Two heterogeneous patterns P1 (Figure 4.3) and P2 (Figure 4.4) were considered for the study. In the first pattern (P1) the domain was filled with three layers of sand with coarse sand (CS), fine sand (FS) and coarse sand (CS). In the second pattern (P2) the layers of Fine sand (FS), coarse sand (CS), and fine sand (FS) were filled. An initial spill of dodecane was established by releasing 573ml of dodecane at 30 cm below the top surface. The release was stopped after 19 hours. The water table in the simulation tank was maintained 15 cm to have a constant head boundaries. The impacts of heterogeneity on LNAPL movement for both the patterns P1 and P2 are described separately.

Table 5.4: Sand medium properties adopted from Oostrom et al. (1999).

Porous medium properties	Coarse sand (CS)	Fine sand (FS)
Brooks-Corey entry head, h_d (cm)	2.3	19.7
Brooks and Corey (λ)	4.3	5.1
Residual water saturation(S_{rw})	0.11	0.14
Permeability, k (10^{-6}) cm^2	1.21	0.021
Porosity(η)	0.34	0.41
Density, ρ (g cm^{-3})	1.749	1.564

5.4.1 The movement of LNAPL in heterogeneous pattern (P1: coarse – fine - coarse sand layers)

Figure 5.11 - 5.13 shows the LNAPL movement for the layered heterogeneity pattern P1 of coarse, fine and coarse sand layers. The capillary fringe of 2.3 cm above water table was used. After 1 hour of spill, just a trace of LNAPL was seen visually below the spill surface. At t=20 hr the maximum amount of LNAPL was observed visually distributed in the fine sand layer providing the lateral spreading of LNAPL. Capillary forces pulled the LNAPL in to the fine sand layer in an unconfined aquifer, where it was held. The LNAPL was thus prevented from reaching capillary fringe. But still some amount of LNAPL was seen visually reaching the capillary fringe just above the layer of coarse sand with saturation of 0.2. At t= 20 hr the fine sand layer in an unconfined aquifer had a maximum LNAPL saturation of approximately 0.4. At t= 24 hr, the vertical movement of LNAPL in coarse sand layer from fine sand layer was observed. Here the LNAPL started to accumulate in capillary fringe region just above the water table and lateral spreading was observed. Still, some of the residual LNAPL was observed above the capillary fringe in fine sand layer. After t=24 hr the LNAPL saturation decreased approximately to 0.3 and started to accumulate in capillary fringe region. The pooling of LNAPL on the top of the water table in the capillary fringe region was clearly visible at t = 36 hr (Figure 5.14) with saturation of 0.3. The horizontal spreading of LANPL was clearly visible moving towards the both ends of simulation tank at t= 36 hr. Finally after t= 48 hr (Figure 5.15), some residual LNAPL was still visible in fine sand layer above capillary fringe whereas the lateral spreading of LNAPL above the water table with constant saturation of 0.3 was clearly visible.
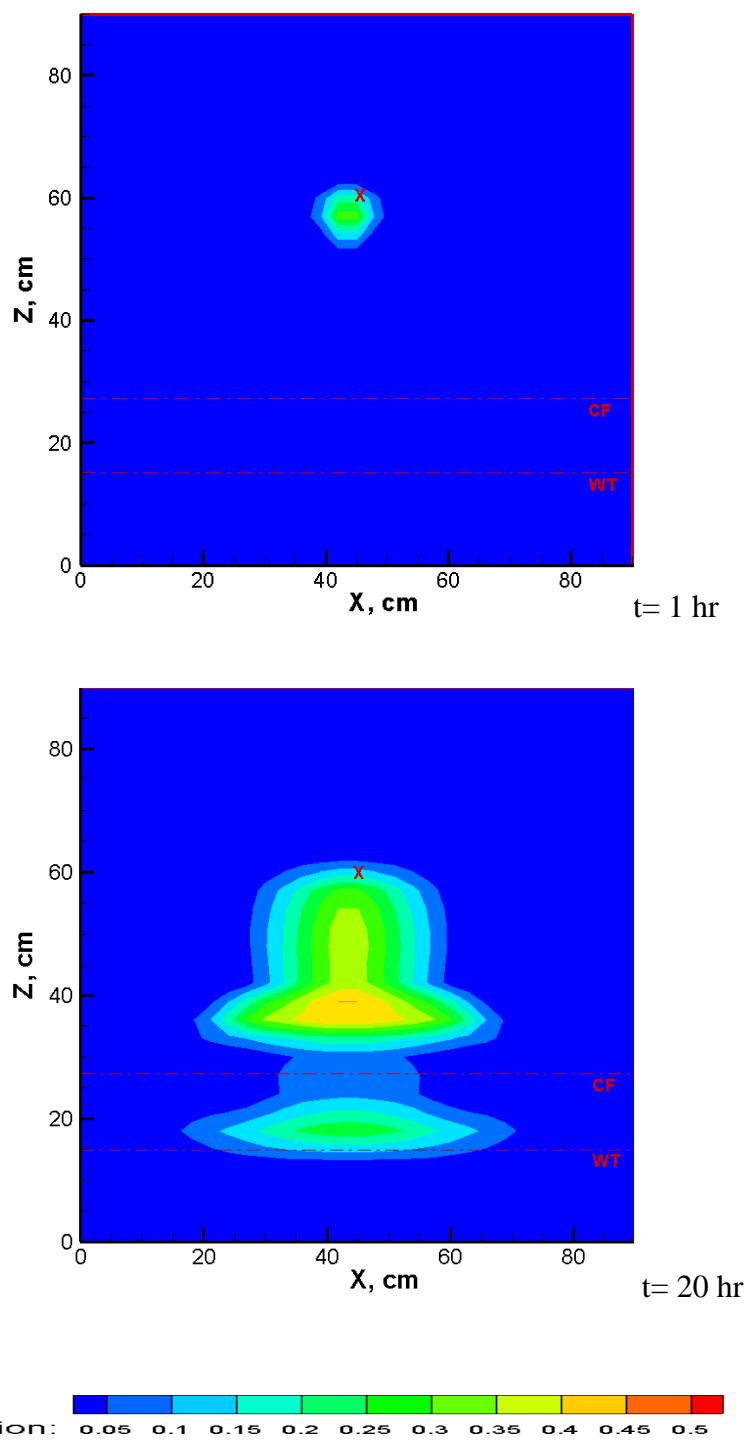
Figure 5.11: Simulation of LNAPL movement in heterogeneous pattern P1 at t= 1 hr and t=20 hr with x= point of release, water table, WT= 15cm, capillary fringe, CF=13 cm, saturation, S=0.1-0.4
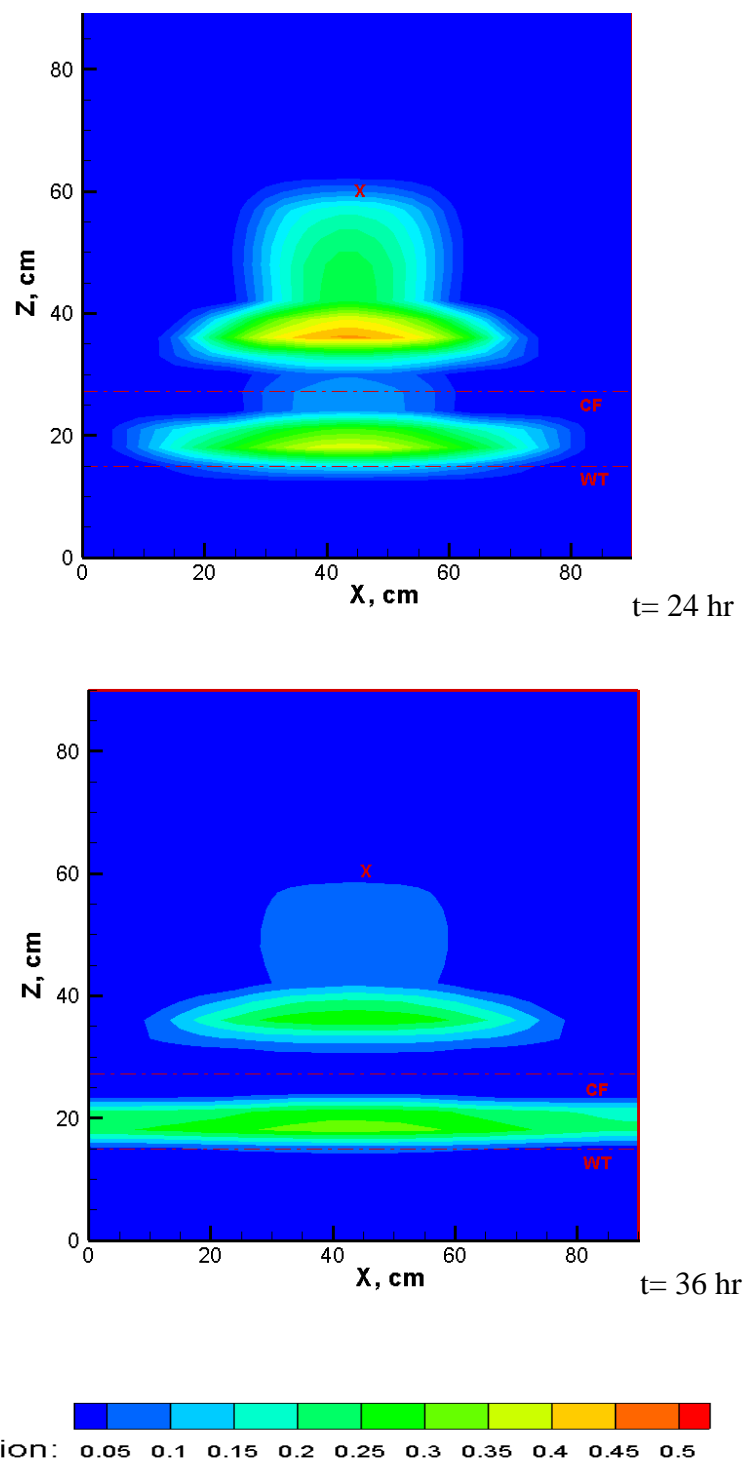
Figure 5.12: Simulation of LNAPL movement in heterogeneous pattern P1 at t= 24 hr and t = 36 hr with saturation, S= 0.3- 0.36
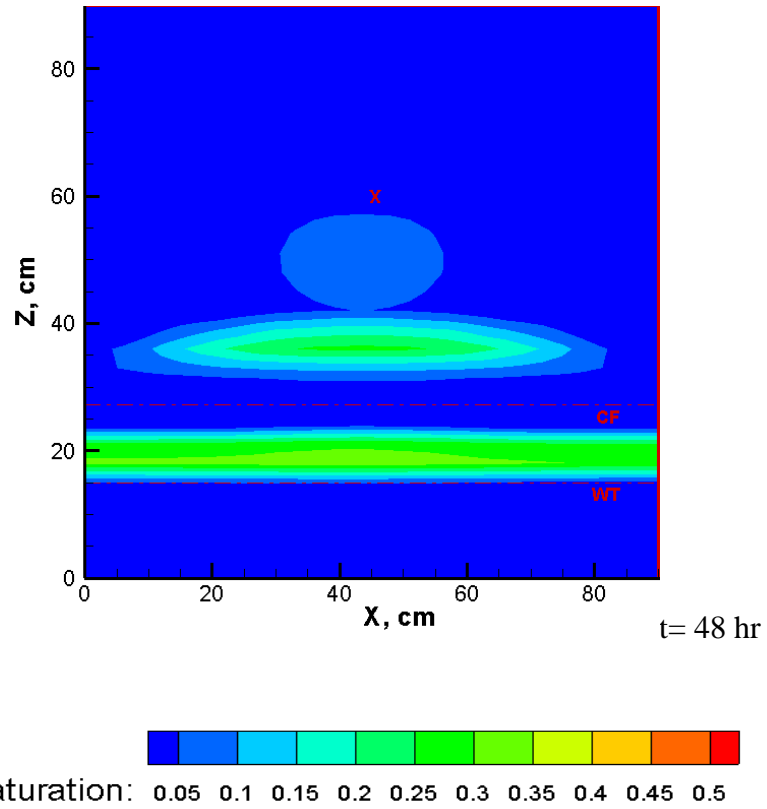
Figure 5.13: Simulation of LNAPL movement in heterogeneous pattern P1 at t = 48 hr with saturation, S= 0.3

5.4.2 The movement of LNAPL in heterogeneous pattern (P2: fine – coarse - fine sand layers)

Figure 5.14 – 5.16 shows the LNAPL distribution for the heterogeneity pattern P2 of fine, coarse and fine sand layer. The capillary fringe of 17.3 cm from water table was used. Simulation was carried out for 48 hr. After 1 hour of spill, the vertical distribution of LNAPL was observed moving faster when compared with Pattern P1. As the coarse sand has a higher conductivity than the fine sand and larger pores than the fine sand, the LNAPL easily penetrate the coarse sand layer thus the initial LNAL vertical distribution was higher in Pattern P2. At t= 20 hr (Figure 5.14), almost all the LNAPL was vertically distributed from coarse sand layer and then LNAPL was accumulated just above the capillary fringe. It then started to move laterally towards the both ends of simulation tank. In the coarse sand layer the vertical movement was faster as that compared to fine sand layer due to the difference in grain size, water saturation and entry pressure; this result can be compared to the result stated by Wipfler et al., (2004). Between t= 24 to 48 hr, the LNAPL was seen trapped the fine sand layer above capillary fringe leaving some residual LNAPL in coarse sand layer. After 48 hr of simulation, comparing the LNAPL movement in both heterogeneous pattern P1(Figure 5.14) and P2 (Figure 5.16), differences in NAPL saturation and pooling of LNAPL due to presence of layered heterogeneity can clearly be predicated regarding their movement in two different porous medium of coarse and fine sand layer.
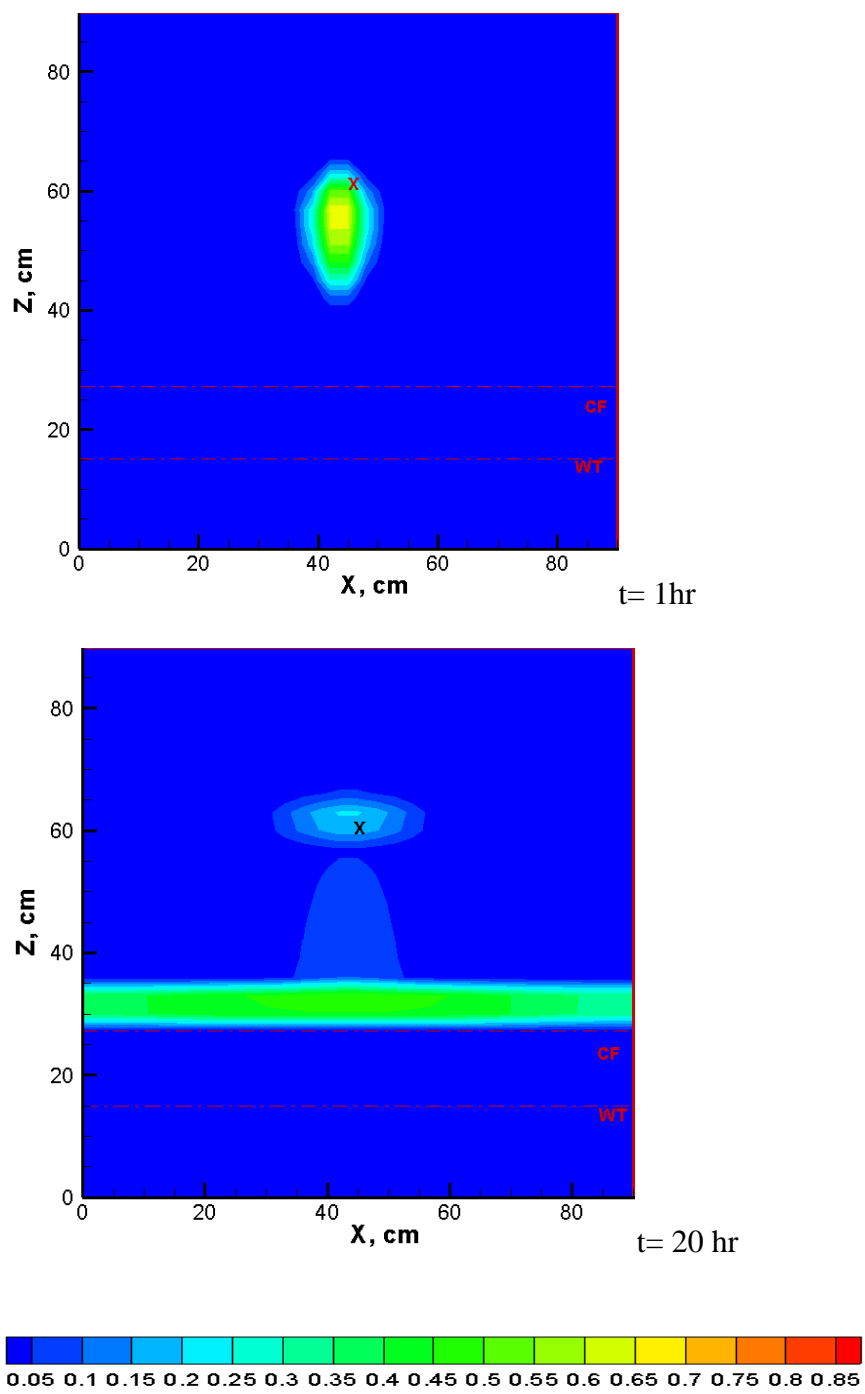
Figure 5.14: Simulation of LNAPL movement in heterogeneous pattern P2 at t = 1hr and t= 20hr with x= point of release, water table WT= 15cm, capillary fringe CF= 13cm, saturation, S= 0.25-0.45
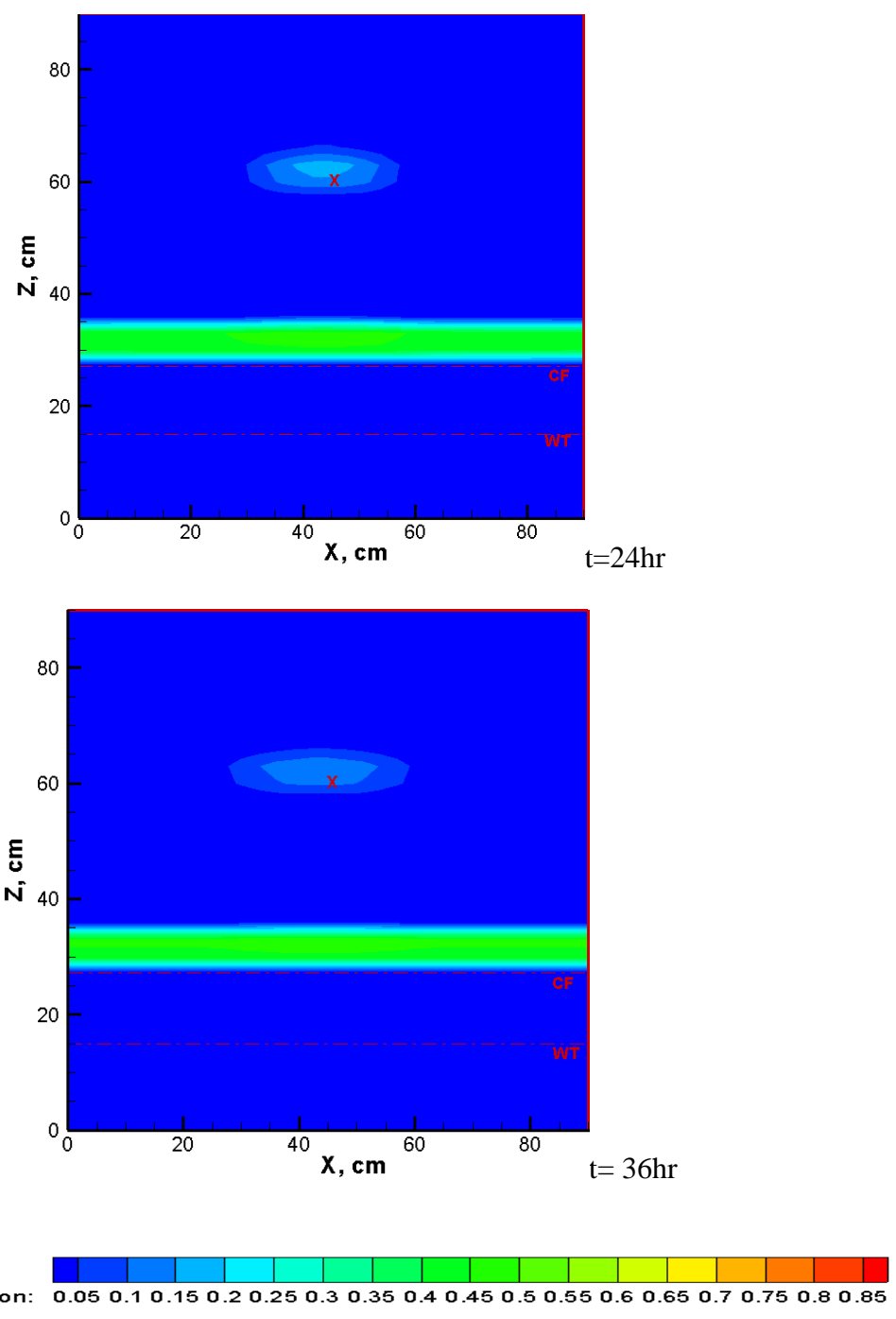
Figure 5.15: Simulation of LNAPL movement in heterogeneous pattern P2 at t =24 hr to t =36 hr with saturation, S= 0.35- 0.45

NAPL Saturation: 0.05 0.1 0.15 0.2 0.25 0.3 0.35 0.4 0.45 0.5 0.55 0.6 0.65 0.7 0.75 0.8 0.85
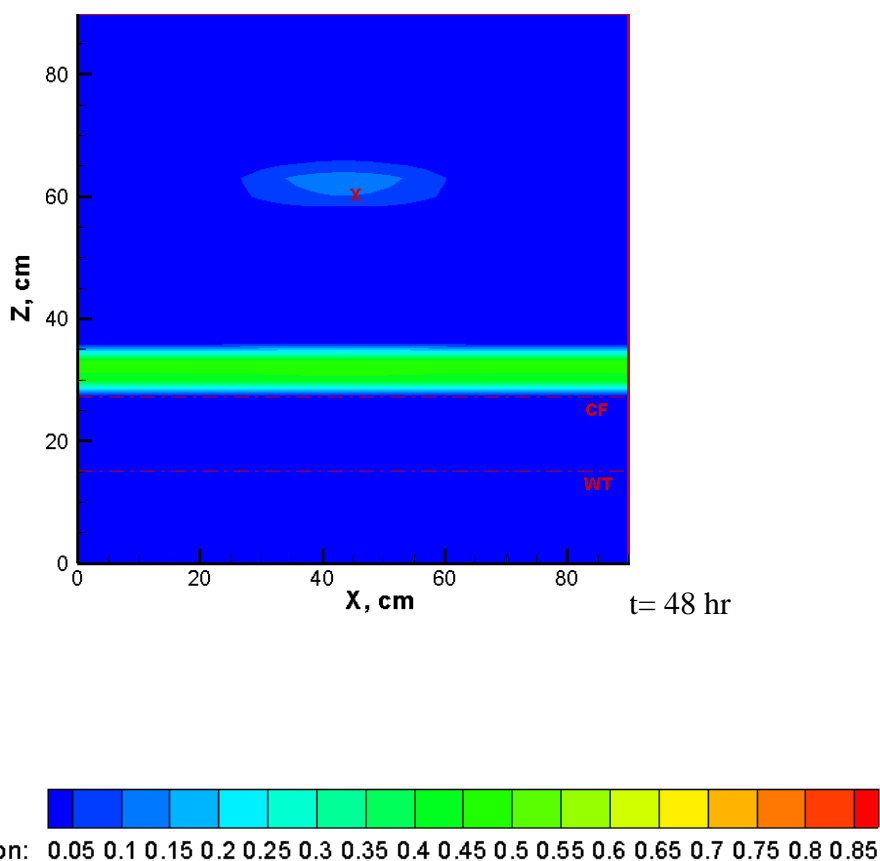
Figure 5.16: Simulation of LNAPL movement in heterogeneous pattern P2 at t = 48 hrs with saturation, S = 0.35-0.45

Figure 5.11- 5.16 shows the distribution of LNAPL plume for two heterogeneous patterns P1 and P2. As seen in the figures, the LNAPL movement and saturation distribution was different for two cases of heterogeneity patterns. In pattern P1 (Figure 5.11- 5.13), the presence of fine sand layer above the capillary fringe caused horizontal spreading of LNAPL in the capillary fringe region whereas in pattern P2 (Figure 5.14-5.16), due to the presence of coarse sand layer just after the LNAPL spill the vertical movement of LNAPL was clearly visible to be moving faster.

The LNAPL infiltrated into the fine sand layer above capillary fringe (Figure 5.14- 5.15), and horizontal spreading of LNAPL was seen above in capillary fringe region above water table. Fine sand layer caused pooling of LNAPL and forced it to move horizontally. As the coarse sand matrix has higher conductivity and higher grain size distribution than fine sand matrix, the vertical movement of LNAPL was visible moving faster as compared to movement in the fine sand layer in an unconfined aquifer. In heterogeneous medium of pattern P1 (Figure 5.11 -5.13), LNAPL infiltrated the fine sand layer and accumulated in capillary fringe region of coarse sand layer. Some residual LNAPL was still observed on fine sand layer whereas the accumulated LNAPL moves laterally towards the both ends on simulation tank above water table. Vertical distribution of LNAPL was less in fine sand medium as compared to coarse sand medium. LNAPL migrates easily in coarse sand medium than in fine sand medium due to larger grain size. Capillary forces play an important role in case of multi- phase fluid flow in layered heterogeneous system. The entry pressure or minimum capillary pressure needed for a non-wetting fluid to enter a porous medium is important for NAPL migration in heterogeneous system. Pantazidou and Sitar (1993) conducted 2-D LNAPL infiltration experiments in unsaturated heterogeneous (layered) as well as homogeneous sand packs. They found that LNAPL movement is largely dependent on the number and horizontal continuity of layers. In general more lateral spreading of LNAPL occurred in the heterogeneous systems than in homogeneous sand pack system (Schroth et al., 1998). Our simulation was mainly focused on impact of heterogeneous medium on LNAPL movement; apart from heterogeneous medium LNAPL movement may mainly depend on the water saturation beneath the release location, NAPL fluid properties, conductivity of porous media, porous media grain size, pore throat displacement entry pressure.

CHAPTER 6

CONCLUSION AND RECOMMENDATION

6.1 Conclusions

The objectives of this research were to study the impact of layered heterogeneity on flow pattern of LNAPL in 2-D numerical simulator using STOMP, and also study the effect of heterogeneity on LNAPL movement and spreading behavior in an unconfined aquifer. Dodecane, a LNAPL was released in an unconfined aquifer for two different heterogeneity patterns (P1: coarse - fine - coarse sand) and pattern (P2: fine – coarse - fine sand). A constant water table head was maintained for numerical simulation of both heterogeneity patterns. The result showed differences on the LNAPL movement between two different heterogeneity patterns P1 and P2. In pattern P1 the horizontal spreading of LNAPL above water table in capillary fringe region was visible whereas in pattern P2 LNAPL distribution did not even reached capillary fringe. The numerical simulation with heterogeneity pattern (P1: coarse -fine - coarse sand) showed that after LNAPL release, the infiltration of LNAPL was visible in fine sand layer where some LNAPL was trapped and finally the LNAPL accumulated in capillary fringe above water table where later spreading was observed. Whereas for pattern (P2: fine – coarse -fine sand) showed that after LNAPL release, the LNAPL was clearly visible migrating faster from coarse sand layer and infiltrating into fine sand layer just above the capillary fringe region. The lateral spreading of LNAPL towards the both ends of simulation tank was visible.

Heterogeneity in soil properties has a significant influence on spreading behavior of LNAPL in soil and groundwater. The presence of small- scale layer of fine-grained sand may

produce localized pools of NAPL after the spreading has stopped as mentioned by (Ataie-Ashtiani et al., 2001). The result also showed that the presence of fine grained sand layer caused the pooling of LNAPL above it. Capillary forces play an important role in the case of multi-phase fluid flow in layered heterogeneous system. The entry pressure that is the minimum capillary pressure needed for a non-wetting fluid to enter a porous medium was higher for fine grain sand. The porous media grain size and its variation between adjacent zones was important factor influencing the NAPL distribution, migration in the heterogeneous system. Numerical simulations were carried out with the water –oil mode of multi-fluid flow simulator STOMP (White & Oostrom, 1996).

6.2 Recommendations

Knowledge gained from this modeling study serve as a basic understanding of LNAPL movement in an unconfined aquifer under layered heterogeneous system. The scope of this research was limited to study the impacts of layered heterogeneity on LNAPL movement in an unconfined aquifer. Hence, the geometry and position of the NAPL pool in the subsurface are important for the effective design of remediation strategies. However, further in depth research should be conducted to investigate the other factors affecting the NAPL movement apart from this research. The following areas need to be investigated:

- Conduct the numerical simulation for more complex pattern of heterogeneity
- Studying the influence of hysteretic effect (entrapment) and effects of fluctuating water table on LNAPL movement
- Model in a large system

REFERENCES

Abriola, L. M., Condit, W. E., and Cowell, M. A. (2000). "Investigation of the Influence of Soil Texture on Rate Limited Micellar Solubilization."*Journal of Environmental Engineering*, 126(1), 39-46.

Abriola, L. M., Drummond, C. D., Hahn, E. J., Hayes, K. F., Kibbey, T. C. G., Lemke, L. D., Pennell, K. D., Petrovskis, E. A., Ramsburg, C. A., and Rathfelder, K. M. (2005). "Pilot-Scale Demonstration of Surfactant-Enhanced PCE Solubilization at the Bachman Road Site. 1. Site Characterization and Test Design." *Environmental Science & Technology*, 39(6), 1778-1790.

Abriola, L. M., and Pinder, G. F. (1985). "A Multiphase Approach to the Modeling of Porous Media Contamination by Organic Compounds: 1. Equation Development." *Water Resour. Res.*, 21(1), 11-18.

Anderson, W. G. (1987). Wettability Literature Survey- Part 5: "The effects of wettability on Relative Permeability." *Journal of Petroleum Engineers*, 1453-1468.

Ataie-Ashtiani, B., Hassanizadeh, S. M., Oostrom, M., Celia, M. A., and White, M. D. (2001). "Effective parameters for two-phase flow in a porous medium with periodic heterogeneities." *Journal of Contaminant Hydrology*, 49(1-2), 87-109.

Benson, D. A. (1994). Users manual to VENT2D: A multicompound vapor transport and phase distribution model. Claremont St, Reno, Nevada.

Brooks, R. H., and Corey, A. T. (1964). "Hydraulic Properties of Porous Media." *Hydrology Papers, Colorado State University* (March).

Center for Petroleum and Geosystems Engineering (2000). Technical documentation for UTCHEM-9, A three- dimensional chemical flood simulator. The University of Texas at Austin: Texas. http://www.cpge.utexas.edu/utchem/UTCHEM_Tech_Doc.pdf.

Chao, W.-L., Parlange, J. Y., and Steenhuis, T. S. (2000). "An Analysis of the Movement of Wetting and Nonwetting Fluids in Homogeneous Porous Media." *Transport in Porous Media*, 41(2), 121-135.

Chevalier, L. R. (1998). "Experimental and numerical evaluation of LNAPL lens and polluted capillary fringe thickness." *Journal of Environmental Engineering,* 124(2*), 156-161.*

Chevalier, L. R., and Petersen, J. (1999). "Literature Review of 2-D Laboratory Experiments in NAPL Flow, Transport, and Remediation." *Journal of Soil Contamination*, 8(1), 149-167.

Corapcioglu, M. Y., and Baehr, A. L. (1987). "A compositional multiphase model for groundwater contamination by petroleum products: 1. Theoretical considerations." *Water Resour. Res.*, 23(1), 191-200.

Das, D., Hassanizadeh, S., Rotter, B., and Ataie-Ashtiani, B. (2004). "A Numerical Study of Micro-Heterogeneity Effects on Upscaled Properties of Two-Phase Flow in Porous Media." *Transport in Porous Media*, 56(3), 329-350.

Dobson, R., Schroth, M. H., and Zeyer, J. (2007). "Effect of water-table fluctuation on dissolution and biodegradation of a multi-component, light non-aqueous- phase liquid." *Journal of Contaminant Hydrology*, 94, 235-248.

Duijn, C. J., Molenaar, J., and Neef, M. J. (1995). "The effect of capillary forces on immiscible two-phase flow in heterogeneous porous media." *Transport in Porous Media*, 21(1), 71-93.

Eckberg, D. K., and Sunada, D. K. (1984). "Nonsteady three-phase immiscible fluid distribution in porous media." *Water Resour. Res.*, 20(12), 1891-1897.

Environmental Protection Agency (2009). National Primary Drinking Water Regulations. May 2009 http:// www.epa.gov/ogwdw/consumer/pdf/mcl.pdf (March 10, 2010).

Gelhar, L. W., Welty, C., and Rehfeldt, K.R. (1992). "A critical review of data on field scale dispersion in aquifers." *Water Resour. Res*., 28, 1955-1974.

Guarnaccia, J., Pinder, G.,and Fishman, M. (1997). "NAPL: Simulator documentation." NRMRL USEPA: Ada, Oklahoma.

Hochmuth, D. P., and Sunada, D. K. (1985). "Groundwater model of two-phase immiscible flow in coarse material." *Ground Water*, 23(5), 617-626.

Host-Madsen, J., and Hogh Jensen, K. (1992). "Laboratory and numerical investigations of immiscible multiphase flow in soil." *Journal of Hydrology*, 135(1-4), 13-52.

Huyakorn, P. S., Wu, Y. S., Pandey, S., and Park, N. S. (1992). "Multiphase Analysis of Groundwater, Non Aqueous Phase Liquid and Soluble Component." *Hydro Geologic Inc*., Herndon, VA.

Illangasekare, T. H., Ramsey Jr, J. L., Jensen, K. H., and Butts, M. B. (1995). "Experimental study of movement and distribution of dense organic contaminants in heterogeneous aquifers." *Journal of Contaminant Hydrology*, 20(1-2), 1-25.

Kaluarachchi, J. J., and Parker, J. C. (1989). "An efficient finite element method for modeling multiphase flow." *Water Resour. Res.*, 25(1), 43-54.

Kaluarachchi, J. J., and Parker, J. C. (1990). "Modeling multicomponent organic chemical transport in three-fluid-phase porous media." *Journal of Contaminant Hydrology*, 5(4), 349-374.

Katyal, A. K., Kaluarachchi, J. J., Parker, J. C., and Cho, J. S. (1991). "A two dimensional finite element program for multiphase flow and multicomponent transport." Program Documentation, Version, RSKERL USEPA: Ada, Oklahoma.

Kechavarzi, C., Soga, K., and Illangasekare, T. H. (2005). "Two-dimensional laboratory simulation of LNAPL infiltration and redistribution in the vadose zone." *Journal of Contaminant Hydrology*, 76(3-4), 211-233.

Kueper, B. H., Abbott, W., and Farquhar, G. (1989). "Experimental observations of multiphase flow in heterogeneous porous media." *Journal of Contaminant Hydrology*, 5(1), 83-95.

Kueper, B. H., and Frind, E. O. (1991). "Two-phase flow in heterogeneous porous media: 1. Model development." *Water Resour. Res.*, 27(6), 1049-1057.

Lenhard, R. J., Johnson, T. G., and Parker, J. C. (1993). "Experimental observations of nonaqueous-phase liquid subsurface movement." *Journal of Contaminant Hydrology*, 12(1-2), 79-101.

Lenhard, R. J., and Parker, J. C. (1988). "Experimental validation of the theory of extending two-phase saturation-pressure relations to three-fluid phase systems for monotonic drainage paths." *Water Resour. Res.*, 24(3), 373-380.

Leverett, M. C. (1941). "Capillary behavior in porous Media." *Trans. AIME*, 142, 341-358.

Lewis, R. W., Schrefler, B. A., and Rahman, N. A. (1998). "A finite element analysis of multiphase immiscible flow in deforming porous media for subsurface systems." *Communications in Numerical Methods in Engineering*, 14(2), 135-149.

Mackay, D. M., and Cherry, J. A. (1989). "Groundwater contamination: pump-and-treat remediation." *Environmental Science & Technology*, 23(6), 630-636.

Mercer, J. W., and Cohen, R. M. (1990). "A review of immiscible fluids in the subsurface: Properties, models, characterization and remediation." *Journal of Contaminant Hydrology*, 6(2), 107-163.

Miller, C. T., Christakos, G., Imhoff, P. T., McBride, J. F., Pedit, J. A., and Trangenstein, J. A. (1998). "Multiphase flow and transport modeling in heterogeneous porous media: challenges and approaches." *Advances in Water Resources*, 21(2), 77-120.

Ng, K.M., Davis, H.T. and Sciven, L.E. (1978). "Visualization of bob mechanics in flow through porous media." *Chemical Engineering Science*, 33, 1009-1017.

Oostrom, M., Dane, J. H., and Wietsma, T. W. (2007). "A Review of Multidimensional, Multifluid, Intermediate-Scale Experiments: Flow Behavior, Saturation Imaging, and Tracer Detection and Quantification." *Vadose Zone Journal*, 6(3), 610-637.

Oostrom, M., Hofstee, C., and Dane, J. H. (1997). "Light Nonaqueous-Phase Liquid Movement in a Variably Saturated Sand." *Soil Sci. Soc. Am. J.*, 61(6), 1547-1554.

Oostrom, M., Hofstee, C., Lenhard, R. J., and Wietsma, T. W. (2003). "Flow behavior and residual saturation formation of liquid carbon tetrachloride in unsaturated heterogeneous porous media." *Journal of Contaminant Hydrology*, 64(1-2), 93-112.

Oostrom, M., Hofstee, C., Walker, R. C., and Dane, J. H. (1999). "Movement and remediation of trichloroethylene in a saturated, heterogeneous porous medium: 2. Pump-and-treat and surfactant flushing." *Journal of Contaminant Hydrology*, 37(1-2), 179-197.

Oostrom, M., Hofstee, C., and Wietsma, T. W. (2006). "Behavior of a Viscous LNAPL Under Variable Water Table Conditions." *Soil and Sediment Contamination: An International Journal*, 15(6), 543-564.

Pantazidou, M., and Sitar, N. (1993). "Emplacement of nonaqueous liquids in the an unconfined aquifer." *Water Resour. Res.*, 29(3), 705-722.

Patankar, S. V. (1980). "Numerical heat transfer and fluid flow." Hemisphere Publishing Corporation, Washington, D. C.

Pennell, K. D., Jin, M., Abriola, L. M., and Pope, G. A. (1994). "Surfactant enhanced remediation of soil columns contaminated by residual tetrachloroethylene." *Journal of Contaminant Hydrology*, 16(1), 35-53.

Pinal, R., Rao, P. S. C., Lee, L. S., Cline, P. V., and Yalkowsky, S. H. (1990). "Cosolvency of partially miscible organic solvents on the solubility of hydrophobic organic chemicals." *Environmental Science & Technology*, 24(5), 639-647.

Pruess, K., Moridis, G. J., and Oldenburg, C. (1999). TOUGH2 Users Guide, Version 2. Lawrence Berkeley National Laboratory, California.

Reible, D. D., Illangasekare, T. H., Doshi, D. V., and Malhiet, M. E. (1990). "Infiltration of Immiscible Contaminants in the Unsaturated Zone." *Ground Water*, 28(5), 685-692.

Reid, R. C., Prausnitz, J. M., and Poling, B. E. (1987). "The Properties of Gases and Liquids." 4th ed. McGraw Hill, 727-729.

Rimmer, A., Parlange, J. Y., Steenhuis, T. S., Darnault, C., and Condit, W. (1996). "Wetting and nonwetting fluid displacements in porous media." *Transport in Porous Media*, 25(2), 205-215.

Saint Aime, R. (2011). "An evaluation of NAPL wettability in 2-D visualization experiments." Master's Thesis. Southern Illinois University Carbondale.

S.A. Kamaruddin, W. N. A. S., N.A. Rahman, M.P. Zakaria, M. Mustaffar and R. Sa`ari.(2011). "A Review of Laboratory and Numerical Simulations of Hydrocarbons Migration in Subsurface Environments." Journal of Environmental Science and Technology,4. 191-214

Schroth, M. H., Istok, J. D., Ahearn, S. J., and Selker, J. S. (1995). "Geometry and position of light nonaqueous-phase liquid lenses in water-wetted porous media." *Journal of Contaminant Hydrology*, 19(4), 269-287.

Schroth, M. H., Istok, J. D., and Selker, J. S. (1998). "Three-phase immiscible fluid movement in the vicinity of textural interfaces." *Journal of Contaminant Hydrology*, 32(1-2), 1-23.

Seyedabbasi, M. A., Farthing, M. W., Imhoff, P. T., and Miller, C. T. (2008). "The influence of wettability on NAPL dissolution fingering." *Advances in Water Resources*, 31(12), 1687-1696.

Simmons, C. S., McBride, J. F., Cary, J. W., and Lenhard, R. J. (1992). "Organic liquid infiltration into unsaturated porous media." Proceedings of the International Conference on Subsurface Contamination by Immiscible Fluids, Calgary, pp: 213-219.

Thomson, N. R., Graham, D. N., and Farquhar, G. J. (1992). "One-dimensional immiscible displacement experiments." *Journal of Contaminant Hydrology*, 10(3), 197-223.

U.S. EPA (Environmental Protection Agency) (2000). Office of Underground Storage Tanks (OUST) semi- annual report 2000. U.S. Environmental Protection Agency, OUST, Washington, D.C.

Van Geel, P. J., and Sykes, J. F. (1994). "Laboratory and model simulations of a LNAPL spill in a variably-saturated sand, 1. Laboratory experiment and image analysis techniques." *Journal of Contaminant Hydrology*, 17(1), 1-25.

Van Geel, P. J., and Sykes, J. F. (1997). "The importance of fluid entrapment, saturation hysteresis and residual saturations on the distribution of a lighter-than-water non-aqueous phase liquid in a variably saturated sand medium." *Journal of Contaminant Hydrology*, 25(3-4), 249-270.

van Genuchten, M. Th. (1980), " A closed form equation for predicting the hydraulic conductivity of unsaturated soils." *Soil Science Society of America Journal*, 44, 892-898.

Waddill, D. W., and Parker, J. C. (1997). "Recovery of light, non-aqueous phase liquid from porous media: laboratory experiments and model validation." *Journal of Contaminant Hydrology*, 27(1-2), 127-155.

West, C. C., and Harwell, J. H. (1992). "Surfactants and subsurface remediation." *Environmental Science & Technology*, 26(12), 2324-2330.

White, M. D., and Oostrom, M. (1996). "STOMP, Subsurface Transport Over Multiple Phases, theory guide." *Pacific Northwest National Laboratory- 11217*.

Wipfler, E. L., Ness, M., Breedveld, G. D., Marsman, A., and van der Zee, S. E. A. T. M. (2004). "Infiltration and redistribution of LNAPL into unsaturated layered porous media." *Journal of Contaminant Hydrology*, 71(1-4), 47-66.

Zhou, W. Z. (2001). "Numerical simulation of two-phase flow in conceptualized fractures." *Environmental Geology*, 40(7), 797-808.

APPENDICES

APPENDIX A

STOMP INPUT FILE

```
#-------------------------------------------------------------
~Simulation Title Card
#-------------------------------------------------------------
1,
Simulation of LNAPL spill in 2-D tank, Homogeneous system
Saroj kandel,
SIUC,
Sep 09,
12:43,
1,
Simulation of NAPL spills in 2D domain,


#-------------------------------------------------------------
~Solution Control Card
#-------------------------------------------------------------
Normal,
Water-Oil,
1,
0,s,7,hr,1,s,1,min,1.25,8,1.e-6,
700,
Variable Aqueous Diffusion,
,


#-------------------------------------------------------------
~Grid Card
#-------------------------------------------------------------
Uniform Cartesian,
30,1,30,
0.03,m,
0.05,m,
0.03,m,


#-------------------------------------------------------------
~Rock/Soil Zonation Card
#-------------------------------------------------------------
1,
Sand,1,30,1,1,1,30,


#-------------------------------------------------------------
~Mechanical Properties Card
#-------------------------------------------------------------
Sand,2640,kg/m^3,0.24,0.24,,,Millington and Quirk,
```

```
#---------------------------------------------------------------
~Hydraulic Properties Card
#---------------------------------------------------------------
Sand,16.5,hc m/day,,,16.5,hc m/day,


#---------------------------------------------------------------
~Saturation Function Card
#---------------------------------------------------------------
72.0,dynes/cm,,,24.90,dynes/cm,
Sand,Brooks and Corey,7.67,cm,1.0,0.3,72.0,dynes/cm,



#---------------------------------------------------------------
~Aqueous Relative Permeability Card
#---------------------------------------------------------------
Sand, Burdine,,


#---------------------------------------------------------------
~NAPL Relative Permeability Card
#---------------------------------------------------------------
Sand,Burdine,,


#---------------------------------------------------------------
~Oil Properties Card
#---------------------------------------------------------------
DODECANE,
170.340,g/mol,263.6,K,489.5,K,658.2,K,
18.2,bar,713.0,cm^3/mol,0.24,0.575,0.0,debyes,
-9.328e+0,1.149e+0,-6.347e-4,1.359e-7,
Equation 1,-9.328e+0,1.149e+0,-6.347e-4,1.359e-7,
Constant,750.0,kg/m^3,
Constant,0.00134,Pa s,
1.37e10,Pa,


#---------------------------------------------------------------
~Initial Conditions Card
#---------------------------------------------------------------
2,
Aqueous Pressure,102647.1251,Pa,0.0,1/m,,,-
9793.5192,1/m,1,45,1,1,1,30,
NAPL Pressure,-1.e9,Pa,,,,,,,1,45,1,1,1,30,
```

```
#-----------------------------------------------------------
~Source card
#-----------------------------------------------------------
1,
NAPL Mass, 15,15,1,1,20,20,2,
0,d,35.17,kg/day,
0.006074,d,35.17,kg/day,



#-----------------------------------------------------------
~Output Options Card
#-----------------------------------------------------------
16,
15,1,20,
15,1,16,
15,1,12,
15,1,14,
15,1,10,
15,1,8,
15,1,6,
15,1,4,
1,1,17,
1,1,13,
1,1,12,
1,1,11,
1,1,10,
1,1,8,
1,1,6,
1,1,4,
1,1,hr,cm,6,6,6,
2,
napl saturation,,
aqueous saturation,,
5,
0.5,hr,
1,hr,
3,hr,
4,hr,
5,hr,
3,
no restart,,
napl saturation,,
aqueous saturation,,
```

```
#------------------------------------------------------------
~Simulation Title Card
#------------------------------------------------------------
1,
Simulation of LNAPL spill in 2-D tank, Heterogeneous System
Saroj kandel,
SIUC,
Sep  15,
12:43,
1,
Simulation of NAPL spills in 2D domain,



#------------------------------------------------------------
~Solution Control Card
#------------------------------------------------------------
Normal,
Water-Oil,
1,
0,s,500,hr,1,s,1,min,1.25,8,1.e-6,
3000,
Variable Aqueous Diffusion,
,



#------------------------------------------------------------
~Grid Card
#------------------------------------------------------------
Uniform Cartesian,
30,1,30,
0.03,m,
0.05,m,
0.03,m,



#------------------------------------------------------------
~Rock/Soil Zonation Card
#------------------------------------------------------------
3,
fine Sand,1,30,1,1,1,10,
coarse Sand,1,30,1,1,11,20,
fine Sand,1,30,1,1,21,30,
```

```
#-----------------------------------------------------------------
~Mechanical Properties Card
#-----------------------------------------------------------------
fine Sand,1745,kg/m^3,0.34,0.34,,,Millington and Quirk,1,30,1,1,1,10,
coarse Sand,1564,kg/m^3,0.41,0.41,,,Millington and Quirk,1,30,1,11,20,
fine Sand,1745,kg/m^3,0.34,0.34,,,Millington and Quirk,1,30,1,1,21,30,


#-----------------------------------------------------------------
~Hydraulic Properties Card
#-----------------------------------------------------------------
coarse Sand,121e-12,m^2,,,121e-12,m^2,
fine Sand,2.1e-12,m^2,,,2.1e-12,m^2,
coarse Sand,121e-9,m^2,,,121e-9,m^2,


#-----------------------------------------------------------------
~Saturation Function Card
#-----------------------------------------------------------------
72.0,dynes/cm,,,24.90,dynes/cm,
coarse Sand,Brooks and Corey,2.3,cm,4.3,0.11,72.0,dynes/cm,,
fine Sand,Brooks and Corey,19.7,cm,5.1,0.14,72.0,dynes/cm,,



#-----------------------------------------------------------------
~Aqueous Relative Permeability Card
#-----------------------------------------------------------------
coarse Sand, Burdine,,
fine sand ,Burdine,,


#-----------------------------------------------------------------
~NAPL Relative Permeability Card
#-----------------------------------------------------------------
coarse Sand, Burdine,,
fine sand, Burdine,,


#-----------------------------------------------------------------
~Oil Properties Card
#-----------------------------------------------------------------
DODECANE,
170.340,g/mol,263.6,K,489.5,K,658.2,K,
18.2,bar,713.0,cm^3/mol,0.24,0.575,0.0,debyes,
-9.328e+0,1.149e+0,-6.347e-4,1.359e-7,
Equation 1,-9.328e+0,1.149e+0,-6.347e-4,1.359e-7,
Constant,750.0,kg/m^3,
Constant,0.00134,Pa s,
1.37e10,Pa,
```

```
#-------------------------------------------------------------
~Initial Conditions Card
#-------------------------------------------------------------
2,
Aqueous Pressure,102647.1251,Pa,0.0,1/m,,,-
9793.5192,1/m,1,30,1,1,1,30,
NAPL Pressure,-1.e9,Pa,,,,,,,1,30,1,1,1,30,


#-------------------------------------------------------------
~Source card
#-------------------------------------------------------------
1,
NAPL Mass, 15,15,1,1,20,20,2,
0,d,0.54,kg/day,
0.795,d,0.54,kg/day,


#-------------------------------------------------------------
~Output Options Card
#-------------------------------------------------------------
28,
15,1,20,
15,1,16,
15,1,12,
15,1,14,
15,1,10,
15,1,8,
15,1,6,
15,1,4,
5,1,20,
5,1,17,
5,1,13,
5,1,19,
5,1,5,
20,1,20,
20,1,17,
20,1,13,
20,1,9,
20,1,5,
1,1,20,
1,1,17,
1,1,13,
1,1,9,
1,1,5,
30,1,20,
30,1,17,
30,1,13,
30,1,9,
30,1,5,
1,1,hr,cm,6,6,6,
2,
napl saturation,,
```

```
aqueous saturation,,
6,
1,hr,
15,hr,
20,hr,
24,hr,
36,hr,
48,hr,
3,
no restart,,
napl saturation,,
aqueous saturation,,


#------------------------------------------------------------
~Simulation Title Card
#------------------------------------------------------------
1,
Simulation of LNAPL spill in 2-D tank, Heterogeneous system
saroj kandel,
SIUC,
Sep 15,
12:43,
1,
Simulation of NAPL spills in 2D domain,


#------------------------------------------------------------
~Solution Control Card
#------------------------------------------------------------
Normal,
Water-Oil,
1,
0,s,500,hr,1,s,1,min,1.25,8,1.e-6,
3000,
Variable Aqueous Diffusion,
,


#------------------------------------------------------------
~Grid Card
#------------------------------------------------------------
Uniform Cartesian,
30,1,30,
0.03,m,
0.05,m,
0.03,m,
```

```
#----------------------------------------------------------------
~Rock/Soil Zonation Card
#----------------------------------------------------------------
3,
coarse Sand,1,30,1,1,1,10,
fine Sand,1,30,1,1,11,20,
coarse Sand,1,30,1,1,21,30,



#----------------------------------------------------------------
~Mechanical Properties Card
#----------------------------------------------------------------
coarse Sand,1745,kg/m^3,0.34,0.34,,,Millington and
Quirk,1,30,1,1,1,10,
fine Sand,1564,kg/m^3,0.41,0.41,,,Millington and Quirk,1,30,1,11,20,
coarse Sand,1745,kg/m^3,0.34,0.34,,,Millington and
Quirk,1,30,1,1,21,30,
#----------------------------------------------------------------
~Hydraulic Properties Card
#----------------------------------------------------------------
coarse Sand,121e-12,m^2,,,121e-12,m^2,
fine Sand,2.1e-12,m^2,,,2.1e-12,m^2,
coarse Sand,121e-9,m^2,,,121e-9,m^2,


#----------------------------------------------------------------
~Saturation Function Card
#----------------------------------------------------------------
72.0,dynes/cm,,,24.90,dynes/cm,
coarse Sand,Brooks and Corey,2.3,cm,4.3,0.11,72.0,dynes/cm,,
fine Sand,Brooks and Corey,19.7,cm,5.1,0.14,72.0,dynes/cm,,



#----------------------------------------------------------------
~Aqueous Relative Permeability Card
#----------------------------------------------------------------
coarse Burdine,,
fine sand ,Burdine,,

#----------------------------------------------------------------
~NAPL Relative Permeability Card
#----------------------------------------------------------------
coarse Sand, Burdine,,
fine sand, Burdine,,


#----------------------------------------------------------------
~Oil Properties Card
#----------------------------------------------------------------
DODECANE,
170.340,g/mol,263.6,K,489.5,K,658.2,K,
18.2,bar,713.0,cm^3/mol,0.24,0.575,0.0,debyes,
-9.328e+0,1.149e+0,-6.347e-4,1.359e-7,
```

```
Equation 1,-9.328e+0,1.149e+0,-6.347e-4,1.359e-7,
Constant,750.0,kg/m^3,
Constant,0.00134,Pa s,
1.37e10,Pa,



#------------------------------------------------------------
~Initial Conditions Card
#------------------------------------------------------------
2,
Aqueous Pressure,102647.1251,Pa,0.0,1/m,,,-
9793.5192,1/m,1,30,1,1,1,30,
NAPL Pressure,-1.e9,Pa,,,,,,,,1,30,1,1,1,30,,



#------------------------------------------------------------
~Source card
#------------------------------------------------------------
1,
NAPL Mass, 15,15,1,1,20,20,2,
0,d,0.54,kg/day,
0.795,d,0.54,kg/day,

#------------------------------------------------------------
~Output Options Card
#------------------------------------------------------------
28,
15,1,20,
15,1,16,
15,1,12,
15,1,14,
15,1,10,
15,1,8,
15,1,6,
15,1,4,
5,1,20,
5,1,17,
5,1,13,
5,1,19,
5,1,5,
20,1,20,
20,1,17,
20,1,13,
20,1,9,
20,1,5,
1,1,20,
1,1,17,
1,1,13,
1,1,9,
1,1,5,
30,1,20,
30,1,17,
```

```
30,1,13,
30,1,9,
30,1,5,
1,1,hr,cm,6,6,6,
2,
napl saturation,,
aqueous saturation,,
6,
1,hr,
15,hr,
20,hr,
24,hr,
36,hr,
48,hr,
3,
no restart,,
napl saturation,,
aqueous saturation,,
```

APPENDIX B

INSTRUCTION FOR EXECUTION OF STOMP SOURCE CODE

In its native form, the STOMP simulator is a collection of files, which contain either global routines or those associated with a particular operational mode. The STOMP simulator is distributed as assembled source coding for a particular operational mode, with the associated files including modules, example input files. The STOMP source is coded in a combination of FORTRAN 77 and FORTRAN 90. Selected operational modes of the STOMP simulator are available for execution on multiple processors. These versions of the simulator are written in pure FORTRAN 90 with imbedded directives that are interpreted by a FORTRAN preprocessor. Compiling the source code into an executable differs between operating systems, compilers, and memory options. In this section the brief Linux/Unix command used for the compilation of STOMP source code using Fortran 90 compiler is presented. The following steps were used for the execution of source code using Unix system.

- The operational mode stomp-w-o (water –oil) was selected as a source code for the simulation.

- A directory called stomp which contains the input file named as (Example 1) and source code stomp-wo was generated and used as a parent directory.

- The directory bin was again generated within this STOMP directory.

- Now the directory was changed to bin.

- In this bin directory the source code stomp-wo was copied

- To create an executable on a Unix system, the following Unix sequence command were used

mkdir stomp

cd stomp

mkdir bin Example1

cd bin

cp ../../stomp-wo

f90 -c allo.f

f90 -c *.f

f90 -o stomp-w.e *.o

rm *.mod *.o *.f

cd ../ Example1

mv output output.pnnl

../bin/stomp-w.e

diff output output output.pnnl (gives different output file as assigned in input)

Once the output is generated, post- processing of the output file can be done with the Perl script *outputTo.pl*. The Perl program transforms the output file into a formatted input for Gnuplot, Grapher, Igor, Matlab, and Tecplot. The minimum command line is

outputTo.pl

after which the user is prompted for the plotting package name, plotting package input file name, STOMP output file name , reference nodes, and reference node variables.

Tecplot was used for the plotting package for this research. The output for 5 hr NAPL satiation is used here for example as plot.5hr. The following command for plotting the output file in tecplot was used:

./ plotTo.pl tecplot.dat plot.5 hr.plt

All the output data for 5 hr is plotted through tecplot. Just click the file *plot.5hr.plt* and tecplot plots the out file for the user.

VITA

Graduate School
Southern Illinois University

Saroj Kandel

sonique_saroj@hotmail.com

Tribhuvan University
Bachelor's Degree, Civil Engineering, March 2008

Thesis Title:
     The Use of STOMP to Evaluate the Impact of Heterogeneity on LNAPL Pool
     Configuration

Major Professor: Dr. Lizette R. Chevalier